

## Dinuclear Cp\* Cobalt Complexes of the 1,2,4,5-Benzenetetrathiolate Bischelating Ligand

Mitsushiro Nomura and Marc Fourmigué\*

Sciences Chimiques de Rennes, UMR 6226 CNRS, Université de Rennes 1, Campus de Beaulieu, 35042 Rennes Cedex, France

Received April 24, 2007

The dinuclear Cp\*Co dithiolene complex [Cp\*Co(btt)CoCp\*] (**1**) is prepared in high yield from the reaction of the bis(dibutyltin) complex of 1,2,4,5-benzenetetrathiolate (btt) with 2 equiv of [Cp\*Co(CO)<sub>2</sub>]. Mononuclear complexes are also obtained from 1,2,4,5-tetrakis(isopropylthio)benzene (**2**) and sodium in pyridine, from benzo[1,2-*d*;4,5-*d'*]bis(1,3-dithiolane-2,6-dione) (**3**) and <sup>t</sup>BuOK in tetrahydrofuran, or from benzo[*d*]-1,3-dithiolane-2-one (**7**) and <sup>t</sup>BuOK to afford respectively **4a**, **4b**, and [Cp\*Co(bdt)] (**6**), while [Cp\*Co(dmit)] (**8**) is obtained by literature methods. The X-ray structures of the dinuclear complex **1** and the mononuclear complexes **4a** and **6** were determined. They are all characterized by Cp\* ··· btt face-to-face intermolecular interactions, leading to a recurrent 4-fold symmetry motif. The cyclic voltammograms of the [Cp\*Co(dithiolene)] complexes performed in CH<sub>2</sub>Cl<sub>2</sub> show reversible Co<sup>III</sup> to Co<sup>II</sup> reduction but irreversible oxidation waves. The large potential difference between the two reduction waves of the bimetallic complex **1** (269 mV) indicates a stable mixed-valence Co<sup>III</sup>–Co<sup>II</sup> state for the reduced [Cp\*Co(btt)CoCp\*]<sup>−</sup> anion. Upon trimethyl phosphite addition, the mono-P(OMe)<sub>3</sub> adduct [1·P(OMe)<sub>3</sub>] exhibits a red shift of the low-energy absorption band to the IR region (856 nm, ε = 13 000 M<sup>−1</sup>·cm<sup>−1</sup>), while [8·P(OMe)<sub>3</sub>] exhibits a 150 nm blue shift. The stability constants of these P(OMe)<sub>3</sub> adducts were determined from UV–vis spectroscopic titration experiments, with, for example, log(*K*/mol<sup>−1</sup>·dm<sup>3</sup>) values of 3.1 and 0.52 for the mono- and bis-adduct of **1**, respectively. The electrochemical investigation of **1** and **8** in excess phosphite shows a strong current enhancement upon oxidation, attributable to the catalytic generation of the radical cation P(OMe)<sub>3</sub><sup>•+</sup>.

### Introduction

The MS<sub>2</sub>C<sub>2</sub> metalladithiolene ring incorporating one metal, two sulfurs, and two unsaturated carbons is a π-conjugated metal chelate ring with 6π electrons.<sup>1</sup> This five-membered metallacycle has an interesting pseudoaromaticity like a six-membered metallabenzene.<sup>2</sup> Such metal dithiolene complexes show chemical reactivity and structural and physical properties due to this pseudoaromaticity: the effect of ring current,<sup>3</sup> the planarity of the metalladithiolene ring for π conjugation,<sup>4</sup>

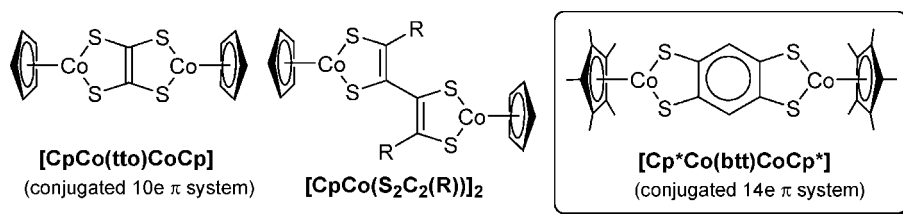
and electrophilic and radical substitution reactions on the ring.<sup>5</sup> These effects concern not only the mono(dithiolene) complexes, formulated as [L<sub>n</sub>M(dithiolene)]<sup>*n*</sup> with formal 6π electrons<sup>6</sup> but also the neutral bis(dithiolene) complexes formulated as [M(dithiolene)<sub>2</sub>]<sup>0</sup> (M = Ni, Pd, Pt) with formal 10π electrons.<sup>7</sup> A further consequence of the π-electron delocalization in metalladithiolene rings is the presence of a low-energy electronic absorption, eventually observed in the near-IR (NIR) region. In fact, the neutral nickel bis(dithiolene) complexes are known to exhibit an electronic absorption in the NIR region (1000–1600 nm) with very strong

\* To whom correspondence should be addressed. E-mail: marc.fourmigue@univ-rennes1.fr. Fax: (+33) 2 23 23 67 32.

- (1) (a) Schrauzer, G. N. *Acc. Chem. Res.* **1969**, *2*, 72. (b) McCleverty, J. A. *Prog. Inorg. Chem.* **1969**, *10*, 49. (c) Sugimori, A. *Yuki Gosei Kagaku Kyokai Shi* **1990**, *48*, 788.  
(2) (a) Bleeke, J. R. *Chem. Rev.* **2001**, *101*, 1205. (b) Wu, H.-P.; Weakley, T. J. R.; Haley, M. M. *Organometallics* **2002**, *21*, 4320. (c) Wu, H.-P.; Lanza, S.; Weakley, T. J. R.; Haley, M. M. *Organometallics* **2002**, *21*, 2824. (d) Iron, M. A.; Lucassen, A. C. B.; Cohen, H.; van der Boom, M. E.; Martin, J. M. L. *J. Am. Chem. Soc.* **2004**, *126*, 11699. (e) Effertz, U.; Englert, U.; Podewils, F.; Salzer, A.; Wagner, T.; Kaupp, M. *Organometallics* **2003**, *22*, 264.

- (3) (a) Boyde, S.; Garner, C. D.; Joule, J. A.; Rowe, D. J. *J. Chem. Soc., Chem. Commun.* **1987**, 800. (b) Gomes, J. A. N. F.; Mallion, R. B. *Chem. Rev.* **2001**, *101*, 1349.  
(4) (a) Rauchfuss, T. B. *Prog. Inorg. Chem.* **2003**, *52*, 1. (b) Fourmigué, M. *Coord. Chem. Rev.* **1998**, *178*, 823.  
(5) (a) Kajitani, M.; Hagino, G.; Tamada, M.; Fujita, T.; Sakurada, M.; Akiyama, T.; Sugimori, A. *J. Am. Chem. Soc.* **1996**, *118*, 489. (b) Sugimori, A.; Tachiya, N.; Kajitani, M.; Akiyama, T. *Organometallics* **1996**, *15*, 5664. (c) Sugimori, A.; Yanagi, K.; Hagino, G.; Tamada, M.; Kajitani, M.; Akiyama, T. *Chem. Lett.* **1997**, 807.

Chart 1



molar absorption coefficient values, up to  $\epsilon = 80\,000\text{ M}^{-1}\text{cm}^{-1}$  in  $[\text{Ni}(\text{R},\text{R}'\text{-timdt})_2]^0$  ( $\text{R},\text{R}'\text{-timdt} = \text{N},\text{N}'\text{-disubstituted imidazolidine-2,4,5-trithione}$ ).<sup>8</sup> Kobayashi also reported that the neutral nickel dithiolene complexes derived from tetrathiafulvalenyldithiolate ligands,<sup>9</sup>  $[\text{Ni}(\text{ptdt})_2]^0$ ,<sup>10</sup>  $[\text{Ni}(\text{tmtdt})_2]^0$ ,<sup>11</sup> and  $[\text{Ni}(\text{hfdt})_2]^0$ ,<sup>12</sup> not only are single-component molecular conductors but also exhibit electronic absorptions in the NIR region due to a very low highest occupied molecular orbital (HOMO)–lowest unoccupied molecular orbital (LUMO) energy gap.<sup>13</sup> An extensive  $\pi$ -electron delocalization is also characteristic of porphyrin and phthalocyanine compounds, and interesting molecular conductivity<sup>14</sup> and low-energy electronic absorptions<sup>15</sup> have been observed in these compounds.

In order to extend the  $\pi$ -electron delocalization of a metalladithiolene ring, two main strategies are conceivable: (1) multinuclear dithiolene complexes based on tetra- or hexadithiolate ligands and (2) delocalization of the dithiolate ligand on a large aromatic group. Dinuclear<sup>16</sup> and even trinuclear<sup>17</sup> nickel dithiolene complexes bridged by the tetrathiooxalate ( $\text{tto}^{4-}$ ) ligand have already been described. These complexes exhibit a very small HOMO–LUMO energy gap attributed to an extensive  $\pi$ -electron delocaliza-

tion. Similarly, a dinuclear cobalt dithiolene complex based on the 1,2,4,5-benzenetetrathiolate ( $\text{btt}^{4-}$ ) ligand, formulated as the dicationic  $[(\text{triphos})\text{Co}(\text{btt})\text{Co}(\text{triphos})]^{2+}$ , shows a low-energy ligand-to-metal charge-transfer transition.<sup>18</sup> The two dithiolene rings are linked here by an aromatic benzene ring.

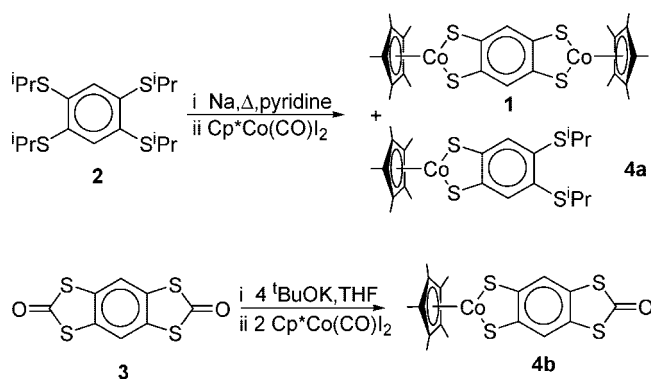
In this work, we have investigated a dinuclear cobalt dithiolene complex with the 14-electron  $\pi$ -conjugated  $\text{btt}^{4-}$  ligand (Chart 1), that is,  $[\text{Cp}^*\text{Co}(\text{btt})\text{CoCp}^*]$  (**1**). Most reported cobalt dithiolene complexes are mononuclear complexes, either heteroleptic monodithiolene complexes, such as  $\text{CpCo}(\text{dithiolene})$ , or homoleptic bis(dithiolene) complexes of the general formula  $[\text{Co}(\text{dithiolene})_2]^{n-}$ .<sup>18–20</sup> Only a few examples of the dinuclear cobalt dithiolene complex have been reported until recently. Guyon et al. have described the dinuclear cobalt dithiolene complexes  $[\text{CpCo}(\text{tto})\text{CoCp}]$  and  $[\text{Cp}^*\text{Co}(\text{tto})\text{CoCp}^*]$ , incorporating the 10-electron  $\pi$ -conjugated  $\text{tto}^{4-}$  ligand (Chart 1).<sup>19</sup> In other dimeric cobalt dithiolene complexes reported by Sugimori et al. and formulated as  $[\text{CpCo}(\text{S}_2\text{C}_2(\text{R}))_2]$  ( $\text{R} = \text{H}, \text{Me}, \text{SiMe}_3, \text{Ph}, p\text{-C}_6\text{H}_4\text{COMe}, p\text{-C}_6\text{H}_4\text{NO}_2$ ),<sup>20</sup> two cobaltadithiolene metal-cycles are linked by a single C–C bond (Chart 1). These are formal  $14\pi$ -electron systems, but the two dithiolene rings are not located on the same plane, hence limiting the extent of conjugation between the two rings.

One general drawback in the handling of such neutral multinuclear dithiolene complexes is their low solubility. For example, the crystal structure and physical properties of  $[\text{CpCo}(\text{tto})\text{CoCp}]$  in solution have not been investigated because of its low solubility.<sup>19</sup> The introduction of the  $\text{Cp}^*$  ligand ( $\eta^5$ -pentamethylcyclopentadienyl) is generally a successful alternative,<sup>21</sup> as illustrated by the reported crystal structures of several dinuclear metal dithiolene complexes with the  $\text{tto}^{4-}$  ligand such as  $[\text{Cp}^*\text{Co}(\text{tto})\text{CoCp}^*]$ ,<sup>22</sup>  $[\text{Cp}^*\text{Ni}(\text{tto})\text{NiCp}^*]$ ,<sup>23</sup>  $[\text{Cp}^*\text{Rh}(\text{tto})\text{RhCp}^*]$ ,<sup>24</sup> or the oxidized complex  $[\text{Cp}^*\text{IrBr}(\text{tto})\text{IrBrCp}^*]$ .<sup>25</sup> A similar strategy has been

- (6) (a) Paw, W.; Cummings, S. D.; Mansour, M. A.; Connick, W. B.; Geiger, D. K.; Eisenberg, R. *Coord. Chem. Rev.* **1998**, *171*, 125. (b) Zuleta, J. A.; Bevilacqua, J. M.; Eisenberg, R. *Coord. Chem. Rev.* **1991**, *111*, 237. (c) Sugimori, A.; Akiyama, T.; Kajitani, M.; Sugiyama, T. *Bull. Chem. Soc. Jpn.* **1999**, *72*, 879.
- (7) Beswick, C. L.; Schulman, J. M.; Stiefel, E. I. *Prog. Inorg. Chem.* **2003**, *52*, 55.
- (8) Aragoni, M. C.; Arca, M.; Demartin, F.; Devillanova, F. A.; Garau, A.; Isaia, F.; Lelj, F.; Lippolis, V.; Verani, G. *J. Am. Chem. Soc.* **1999**, *121*, 7098.
- (9) Abbreviations: ptdt = propylenedithiotetrathiafulvalenedithiolate, tmtdt = trimethylenetetrathiafulvalenedithiolate, hfdt = bis(trifluoromethyl)tetrathiafulvalenedithiolate.
- (10) (a) Kobayashi, A.; Tanaka, H.; Kumasaki, M.; Torii, H.; Narymbetov, B.; Adachi, T. *J. Am. Chem. Soc.* **1999**, *121*, 10763. (b) Kobayashi, A.; Tanaka, H.; Kobayashi, H. *J. Mater. Chem.* **2001**, *11*, 2078. (c) Kumasaki, M.; Tanaka, H.; Kobayashi, A. *J. Mater. Chem.* **1998**, *8*, 301.
- (11) (a) Tanaka, H.; Okano, Y.; Kobayashi, H.; Suzuki, W.; Kobayashi, A. *Science* **2001**, *291*, 285. (b) Kobayashi, A.; Tanaka, H.; Kobayashi, H. *J. Mater. Chem.* **2001**, *11*, 2078. (c) Tanaka, H.; Tokumoto, M.; Ishibashi, S.; Graf, D.; Choi, E. S.; Brooks, J. S.; Yasuzuka, S.; Okano, Y.; Kobayashi, H.; Kobayashi, A. *J. Am. Chem. Soc.* **2004**, *126*, 10518. (d) Kobayashi, A.; Zhou, B.; Kobayashi, H. *J. Mater. Chem.* **2005**, *15*, 3449.
- (12) Sasa, M.; Fujiwara, E.; Kobayashi, A.; Ishibashi, S.; Terakura, K.; Okano, Y.; Fujiwara, H.; Kobayashi, H. *J. Mater. Chem.* **2005**, *15*, 155.
- (13) Kobayashi, A.; Sasa, M.; Suzuki, W.; Fujiwara, E.; Tanaka, H.; Tokumoto, M.; Okano, Y.; Fujiwara, H.; Kobayashi, H. *J. Am. Chem. Soc.* **2004**, *126*, 426.
- (14) (a) Inabe, T.; Tajima, H. *Chem. Rev.* **2004**, *104*, 5503. (b) Ogawa, M. Y.; Martinsen, J.; Palmer, S. M.; Stanton, J. L.; Tanaka, J.; Greene, R. L.; Hoffman, B. M.; Ibers, J. A. *J. Am. Chem. Soc.* **1987**, *109*, 1115. (c) Hoffman, B. M.; Ibers, J. A. *Acc. Chem. Res.* **1983**, *16*, 15.
- (15) Tsuda, A.; Osuka, A. *Science* **2001**, *293*, 79.

- (16) (a) Pullen, A. E.; Zeltner, S.; Olk, R.-M.; Hoyer, E.; Abboud, K. A.; Reynolds, J. R. *Inorg. Chem.* **1996**, *35*, 4420. (b) Pullen, A. E.; Zeltner, S.; Olk, R.-M.; Hoyer, E.; Abboud, K. A.; Reynolds, J. R. *Inorg. Chem.* **1997**, *36*, 4163. (c) Pullen, A. E.; Abboud, K. A.; Reynolds, J. R.; Piotraschke, J.; Zeltner, S.; Olk, R.-M.; Hoyer, E.; Liu, H. L.; Tanner, D. B. *Synth. Met.* **1997**, *86*, 1791.
- (17) Kubo, K.; Nakao, A.; Yamamoto, H. M.; Kato, R. *J. Am. Chem. Soc.* **2006**, *128*, 12358.
- (18) Heinze, K.; Huttner, G.; Zsolnai, L. *Z. Naturforsch. B: Chem. Sci.* **1999**, *54*, 1147.
- (20) Akiyama, T.; Amino, M.; Saitou, T.; Utsunomiya, K.; Seki, K.; Ikoma, Y.; Kajitani, M.; Sugiyama, T.; Shimizu, K.; Sugimori, A. *Bull. Chem. Soc. Jpn.* **1998**, *71*, 2351.
- (21) (a) Mori, H.; Nakano, M.; Tamura, H.; Matsubayashi, G. *J. Organomet. Chem.* **1999**, *574*, 77. (b) Mori, H.; Nakano, M.; Tamura, H.; Matsubayashi, G. *Chem. Lett.* **1998**, 729.
- (22) Englert, M. H. Ph.D. Dissertation, University of Wisconsin, Madison, WI, 1983.

## Scheme 1



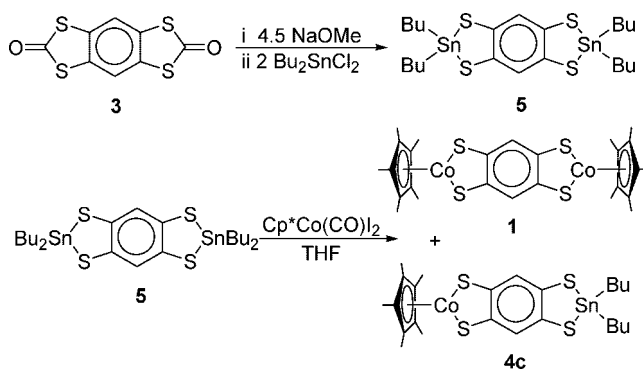
used here, and we report in this paper the preparation and structural and electronic properties of the dinuclear cobalt dithiolene complex with  $\text{btt}^{4-}$  and  $\text{Cp}^*$  ligands, that is, compound **1**, which incorporates an attractive 14-electron  $\pi$ -conjugated system. The related mononuclear benzene-1,2-dithiolate  $\text{Cp}^*\text{Co}(\text{bdt})$ , was also prepared for comparison purposes.

Such  $[\text{CpM}(\text{dithiolene})]$  ( $\text{M} = \text{Co}, \text{Rh}, \text{Ir}$ ) complexes with a Cp ring instead of a  $\text{Cp}^*$  one are also known to present a coordinative unsaturation on the central metal associated with its formal 16-electron count. The chemical reactivity of these  $[\text{CpCo}(\text{dithiolene})]$  complexes has been extensively investigated by Sugimori and Kajitani, leading to the formation of 18-electron adducts by the addition of phosphine or phosphite to the central metal,<sup>26</sup> alkylidene,<sup>27</sup> imido,<sup>28</sup> alkyne,<sup>29</sup> and quadricyclane to the metal–sulfur bond.<sup>30</sup> This type of reactivity has not been investigated in the corresponding  $\text{Cp}^*$  complexes, while the electron-donating character of the  $\text{Cp}^*$  versus Cp ring might lower the reactivity of such  $[\text{Cp}^*\text{Co}(\text{dithiolene})]$  complexes. We report here the first investigation in this direction, based on the addition reaction of  $\text{P}(\text{OMe})_3$  to several  $[\text{Cp}^*\text{Co}(\text{dithiolene})]$  complexes, with the determination of the association constants ( $K$ ) and the molecular structures of these  $\text{P}(\text{OMe})_3$  adducts, together with electrochemical investigations showing that these complexes can act as electron mediators for the oxidation of phosphite through a catalytic process.

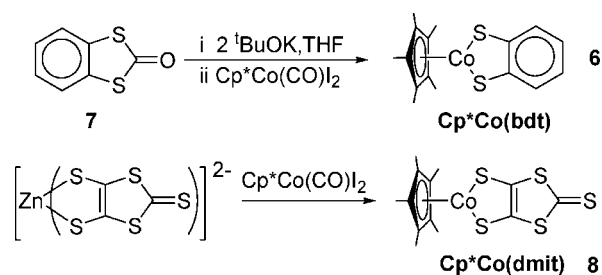
## Results and Discussion

**Preparations and Molecular Structures.** Several methods for the preparation of the dinuclear  $\text{Cp}^*\text{Co}$  dithiolene complex **1** were attempted depending on the available btt

## Scheme 2



## Scheme 3



sources needed for reaction with the air-stable  $\text{Co}^{\text{III}}$   $[\text{Cp}^*\text{Co}(\text{CO})_2]$  species. 1,2,4,5-Benzenetetrathiol itself is very air-sensitive, particularly in the presence of bases.<sup>31</sup> Three different starting materials were thus considered as precursors of the needed btt. The 1,2,4,5-tetrakis(isopropylthio)benzene (**2**) was obtained from 1,2,4,5-tetrachlorobenzene and isopropyl thiolate in hexamethylphosphoric acid triamide (HMPA) or *N,N*-dimethylformamide.<sup>32,33</sup> It can be deprotected by treatment with sodium in hot pyridine to give the  $\text{btt}^{4-}$  tetrathiolate<sup>33,34</sup> or reacted with phosgene to afford a protected form as bis(dithiocarbonate),<sup>33</sup> i.e., the benzo[1,2-*d*;4,5-*d'*]bis(1,3-dithiolane-2,6-dione) (**3**). The latter is easily deprotected with strong bases such as sodium methanolate in MeOH or sodium *tert*-amylate in tetrahydrofuran (THF).

Accordingly, the product of the reaction of **2** with sodium in pyridine at 100 °C was treated with 2 equiv of  $[\text{Cp}^*\text{Co}(\text{CO})_2]$  (Scheme 1). Column chromatography separation afforded the dinuclear complex **1** together with the mononuclear complex **4a** in 33% and 27% yields, respectively. On the other hand, when the  $\text{btt}^{4-}$  tetraanion was generated from **3** and  $\text{tBuOK}$  (4 equiv) in THF, the reaction with  $[\text{Cp}^*\text{Co}(\text{CO})_2]$  gave only the mononuclear complex **4b** in 23% yield (Scheme 2), without traces of the binuclear complex **1**.

We therefore envisioned an alternative synthetic procedure based on neutral derivatives of  $\text{btt}^{4-}$  that can function as masked dithiolate sources. Indeed, several neutral organometallic dithiolene derivatives have already been described

- (23) Maj, J. J.; Rae, A. D.; Dahl, L. F. *J. Am. Chem. Soc.* **1982**, *104*, 4278.  
 (24) Holloway, G. A.; Rauchfuss, T. B. *Inorg. Chem.* **1999**, *38*, 3018.  
 (25) Kawabata, K.; Nakano, M.; Tamura, H.; Matsubayashi, G. *Inorg. Chim. Acta* **2004**, *357*, 4373.  
 (26) (a) Henderson, S. D.; Stephenson, T. A.; Wharton, E. J. *J. Organomet. Chem.* **1979**, *179*, 43. (b) Kajitani, M.; Igarashi, A.; Hatano, H.; Akiyama, T.; Sugimori, A.; Matsumoto, S.; Iguchi, Y.; Boennemann, H.; Shimizu, K.; Satō, G. P. *J. Organomet. Chem.* **1995**, *485*, 31.  
 (27) Takayama, C.; Kajitani, M.; Sugiyama, T.; Sugimori, A. *J. Organomet. Chem.* **1998**, *563*, 161.  
 (28) Nomura, M.; Yagisawa, T.; Takayama, C.; Sugiyama, T.; Yokoyama, Y.; Shimizu, K.; Sugimori, A.; Kajitani, M. *J. Organomet. Chem.* **2000**, *611*, 376.  
 (29) Kajitani, M.; Suetsugu, T.; Takagi, T.; Akiyama, T.; Sugimori, A.; Aoki, K.; Yamazaki, H. *J. Organomet. Chem.* **1995**, *487*, C8.

- (30) Nomura, M.; Hatano, H.; Fujita, T.; Eguchi, Y.; Abe, R.; Yokoyama, M.; Takayama, C.; Akiyama, T.; Sugimori, A.; Kajitani, M. *J. Organomet. Chem.* **2004**, *689*, 993.  
 (31) Dirk, C. W.; Cox, S. D.; Wellman, D. E.; Wudl, F. *J. Org. Chem.* **1985**, *50*, 2395.  
 (32) Maiolo, F.; Testaferri, L.; Tiecco, M.; Tingoli, M. *J. Org. Chem.* **1980**, *46*, 3070.  
 (33) Larsen, J.; Bechgaard, K. *J. Org. Chem.* **1987**, *52*, 3285.

such as the titanocene Cp<sub>2</sub>Ti(dithiolene) or the dialkyltin <sup>n</sup>Bu<sub>2</sub>Sn(dithiolene) complexes. These two classes of compounds react directly with electrophiles without the need for generation of the “naked” dithiolate derivative, affording often much “cleaner” reactions with the formation of a neutral, eventually volatile, byproduct such as Cp<sub>2</sub>TiX<sub>2</sub> or <sup>n</sup>Bu<sub>2</sub>SnX<sub>2</sub> (X = Cl, Br, I). Because the bis(titanocene) derivative of btt<sup>4-</sup> is poorly soluble,<sup>35</sup> we considered the still unknown bis(dibutyltin) neutral derivative of btt<sup>4-</sup> (**5**), which was expected to be soluble in common solvents. Furthermore, these tin derivatives have proven to be very efficient dithiolate analogues in the synthesis of tetrathiafulvalenes<sup>36</sup> as well as dithiolate transfer agents for the preparation of dithiolene complexes.<sup>37,38</sup> As shown in Scheme 2, the reaction of **3** with 4.5 equiv of NaOMe in MeOH, followed by the addition of <sup>n</sup>Bu<sub>2</sub>SnCl<sub>2</sub>, afforded the bis(dibutyltin) derivative **5** in 75% yield as an air-stable colorless solid. Its reaction with 2 equiv of [Cp\*Co(CO)I<sub>2</sub>] without any added base afforded cleanly the bimetallic complex **1** in very good yield (78%). The same reaction performed with only 1 equiv of [Cp\*Co(CO)I<sub>2</sub>] afforded a mixture of the bimetallic complex **1** with the heterodinuclear complex **4c** in 50% and 21% yields, respectively (Scheme 2). The high reaction yield obtained with the tin derivative **5**, combined with an easy workup because the only byproduct is a neutral <sup>n</sup>Bu<sub>2</sub>SnI<sub>2</sub> easily separated by chromatography, confirms that these tin dithiolene derivatives are very useful intermediates for the preparation of dithiolene complexes.

In addition, for comparison purposes, the mononuclear complex [Cp\*Co(bdt)] (**6**; bdt = 1,2-benzenedithiolate)<sup>39</sup> was also synthesized (Scheme 3) from [Cp\*Co(CO)I<sub>2</sub>] with benzo[*d*]-1,3-dithiolane-2-one (**7**) in the presence of <sup>t</sup>BuOK (59% yield), while [Cp\*Co(dmit)] (**8**; dmit = 1,3-dithiol-2-thione-4,5-dithiolate) was prepared by a literature method from the zinc complex [Et<sub>4</sub>N]<sub>2</sub>[Zn(dmit)<sub>2</sub>].<sup>40</sup>

The molecular and solid-state structure of the bimetallic complex **1** has been determined by single crystal X-ray diffraction (Figure 1), together with those of the monometallic complexes **4a** and **6** (Figure 2). Selected bond lengths and angles are summarized in Table 1.

(34) Dirk, C. W.; Cox, S. D.; Wellman, D. E.; Wudl, F. *J. Org. Chem.* **1985**, *50*, 2395.

(35) Köpf, H.; Balz, J. *J. Organomet. Chem.* **1990**, *387*, 77.

(36) (a) Yamada, J.; Tanaka, S.; Segawa, J.; Hamasaki, M.; Hagiya, K.; Anzai, H.; Nishikawa, H.; Ikemoto, I.; Kikuchi, K. *J. Org. Chem.* **1998**, *63*, 3952. (b) Yamada, J.; Nishimoto, Y.; Tanaka, S.; Nakanishi, R.; Hagiya, K.; Anzai, H. *Tetrahedron Lett.* **1995**, *36*, 9509. (c) Yamada, J.; Satoki, S.; Mishima, S.; Akashi, N.; Takahashi, K.; Masuda, N.; Nishimoto, Y.; Takasaki, S.; Anzai, H. *J. Org. Chem.* **1996**, *61*, 3987. (d) Yamada, J.; Amano, Y.; Takasaki, S.; Nakanishi, R.; Matsumoto, K.; Satoki, S.; Anzai, H. *J. Am. Chem. Soc.* **1995**, *117*, 1149.

(37) Velazquez, C. S.; Baumann, T. F.; Olmstead, M. M.; Hope, H.; Barrett, A. G. M.; Hoffman, B. M. *J. Am. Chem. Soc.* **1993**, *115*, 9997.

(38) (a) Cerrada, E.; Fernández, E. J.; Gimeno, M. C.; Laguna, A.; Laguna, M.; Terroba, R.; Villacampa, M. D. *J. Organomet. Chem.* **1995**, *492*, 105. (b) Cerrada, E.; Fernández, E. J.; Jones, P. G.; Laguna, A.; Laguna, M.; Terroba, R. *Organometallics* **1995**, *14*, 5537. (c) Cerrada, E.; Laguna, M.; Sorolla, P. A. *Polyhedron* **1997**, *17*, 295.

(39) Kajitani, M.; Fujita, T.; Okumachi, T.; Yokoyama, M.; Hatano, H.; Ushijima, H.; Akiyama, T.; Sugimori, A. *J. Mol. Catal.* **1992**, *77*, L1.

**Table 1.** Selected Bond Lengths (Å), Angles (deg), and Dihedral Angles (deg) of the Structurally Characterized Cp\*Co Dithiolene Complexes

complex	<b>1</b>	<b>4a<sup>a</sup></b>	<b>6</b>
Bond Length			
Co1–S1	2.1330(13)	2.1219(17)	2.1316(5)
Co1–S2	2.1331(13)	2.1199(16)	2.1256(5)
S1–C1	1.752(5)	1.740(5)	1.7425(17)
S2–C2	1.751(5)	1.736(5)	2.1256(5)
C1–C2	1.411(6)	1.396(7)	1.403(2)
Bond Angle			
S1–Co1–S2	92.89(5)	92.56(6)	92.217(19)
Co1–S1–C1	104.66(16)	104.71(19)	105.00(6)
Co1–S2–C2	105.07(16)	105.28(19)	105.21(6)
S1–C1–C2	119.1(3)	119.1(4)	118.54(13)
S2–C2–C1	118.3(3)	118.3(4)	118.40(14)
Cp*/dithiolene dihedral angle	88.65, 89.35	89.35	86.07(4)

<sup>a</sup> Data from one of two independent molecules.

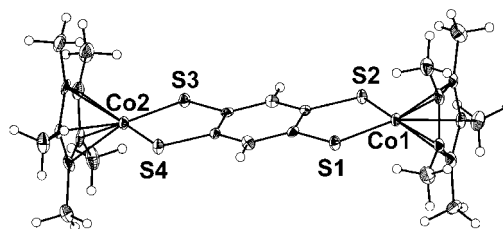


**Figure 1.** ORTEP drawing of the dinuclear Cp\*Co dithiolene complex **1**. X-ray data were collected at 100 K; thermal ellipsoids are drawn at the 50% probability level.

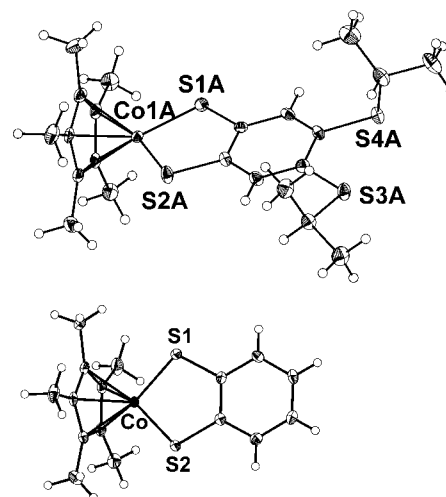


**Figure 2.** ORTEP drawings of **4a** (top, at 100 K) and **6** (bottom, at 100 K). The thermal ellipsoids are drawn at the 50% probability level. Only one of two independent molecules in **4a** is shown.

All complexes exhibit the typical two-legged piano-stool geometry because the dihedral angles between Cp\* and CoS<sub>2</sub> planes are almost 90° (Table 1). The five-membered cobaltadithiolene metallacycles are planar. The Co–S bond lengths in [Cp\*Co(dithiolene)] complexes (Table 1) are slightly longer than those in previously reported CpCo dithiolene complexes, [CpCo(S<sub>2</sub>C<sub>2</sub>R<sub>2</sub>)] (R = CN, COOMe, Ph), where they amount to 2.108–2.110 Å.<sup>27</sup> This is a consequence of the strong electron-releasing effect of the Cp\* substituents,

(40) (a) Ushijima, H.; Sudoh, S.; Kajitani, M.; Shimizu, K.; Akiyama, T.; Sugimori, A. *Appl. Organomet. Chem.* **1991**, *5*, 221. (b) Ushijima, H.; Sudoh, S.; Kajitani, M.; Shimizu, K.; Akiyama, T.; Sugimori, A. *Inorg. Chim. Acta* **1990**, *175*, 11.

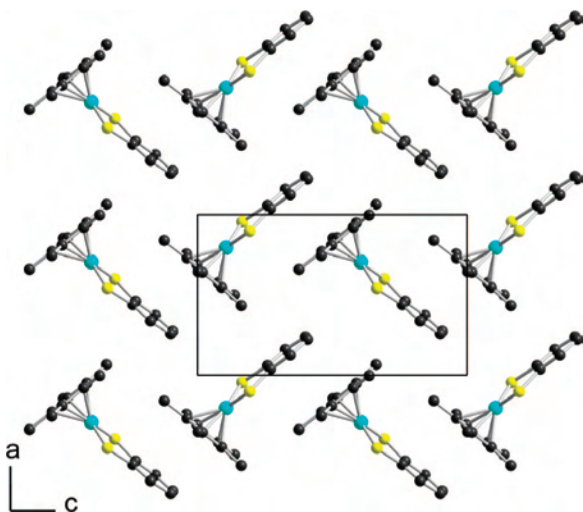


**Figure 3.** Projection view along the *c* axis of one layer of  $[\text{Cp}^*\text{Co}(\text{bdt})]$  molecules **6** showing the face-to-face  $\text{Cp}^*\text{-bdt}$  interaction.

when compared with the Cp ring. Note also that the complexes described here all exhibit a monomeric structure, while similar  $[\text{CpM}(\text{dithiolene})]$  complexes often adopt a dimeric structure<sup>41</sup> with one S atom of the metallacycle entering the coordination sphere of the metal atom of a neighboring molecule. For example,  $[\text{CpCo}(\text{bdt})]$  is known to crystallize as a dimer  $[\text{CpCo}(\text{bdt})]_2$  at room temperature, with a single crystal-to-single crystal phase transition at 150 °C to the monomeric form.<sup>42</sup> Even with the more sterically demanding ( $\eta^6\text{-C}_6\text{H}_6$ ) or  $\text{Cp}^*$  rings, dimeric structures have also been observed, by solution NMR, in  $[(\eta^6\text{-C}_6\text{H}_6)\text{Ru}(\text{bdt})]_2$ ,<sup>43</sup> in the solid state in  $[\text{Cp}^*\text{Rh}(\text{bdt})]_2$ .<sup>44</sup> Surprisingly here, the four structurally characterized  $\text{Cp}^*\text{Co}$  complexes are monomer in the crystal. This is perhaps attributable to the very specific solid-state organizations that those complexes adopt in the crystal.

Indeed, if we first consider **6**, it crystallizes in the orthorhombic system, space group  $P2_12_12_1$ , with one molecule in the general position in the unit cell. The molecules organize into layers in the *ac* plane, with the  $\text{Cp}^*$  ring of one complex almost parallel to the bdt ring (Figure 3) with the shortest  $\text{C}_{\text{Cp}^*}\text{-C}_{\text{bdt}}$  intermolecular distance at 3.40(2) Å, giving rise to the formation of chains running along the *c* axis through this  $\text{Cp}^*\text{-bdt}$  face-to-face interaction.

A similar  $\text{Cp}^*\text{-btt}$  intermolecular interaction is further identified in the solid-state organization of **4a**, which crystallizes in the monoclinic system, space group  $P2_1/c$ , with two crystallographically independent molecules, both in the general position in the unit cell. As shown in Figure 4, the intermolecular  $\text{Cp}^*\text{-btt}$  interaction leads to the formation of

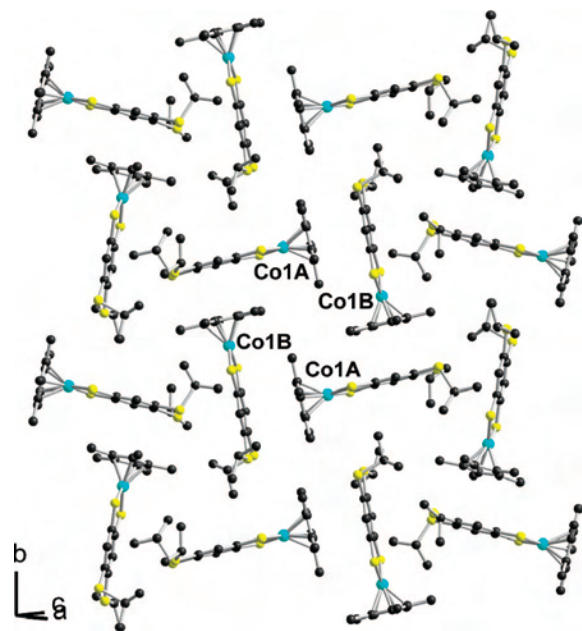


**Figure 4.** Projection view of one layer of complexes **4a** showing the tetrameric motif formed by two A molecules and two B molecules through four  $\text{Cp}^*\text{-btt}$  interactions. The shortest  $\text{C}_{\text{Cp}^*}\text{-C}_{\text{btt}}$  intermolecular distances amount to 3.635(8) and 3.660(8) Å for the  $\text{Cp}^*\text{A-btt}_\text{B}$  and  $\text{Cp}^*\text{B-btt}_\text{A}$  interactions, respectively.

a supramolecular tetrameric motif, isolated from the neighboring ones by the flexible thioisopropyl groups.

This solid-state organization of **6** and **4a** contrasts with the situation usually observed in similar  $[\text{CpM}(\text{dithiolene})]$  complexes, where it most often derives from  $\text{S}\cdots\text{S}$  intermolecular contacts<sup>45</sup> rather than  $\pi\text{-}\pi$  interactions, as observed, for example, in  $[\text{CpCo}(\text{dmit})]$  or  $[\text{Cp}^*\text{Co}(\text{dmit})]$ .<sup>46</sup> It is only recently that such intermolecular  $\text{Cp}\cdots\text{Cp}$  face-to-face interactions have been identified in paramagnetic, formally  $\text{Ni}^{\text{III}}$  species such as  $[\text{CpNi}(\text{bdt})]$ <sup>47</sup> or  $[\text{CpNi}(\text{adt})]$  ( $\text{adt} = \text{acrylonitrile-1,2-dithiolate}$ ),<sup>48</sup> while a cobalt dithiolene complex bearing a tosyl group,  $[(\text{C}_5\text{H}_4\text{NRTs})\text{Co}(\text{S}_2\text{C}_2(\text{CO}_2\text{Me})_2)]$  ( $\text{Ts} = p\text{-toluenesulfonyl}$ ;  $\text{R} = \text{H, Me}$ ), also exhibits intermolecular dithiolene  $\cdots$  dithiolene and dithiolene  $\cdots$  benzene and intramolecular dithiolene  $\cdots$  benzene interactions.<sup>49</sup> The efficiency of these  $\text{Cp}^*\text{-btt}$  interactions is further evidenced in the solid-state organization of the bimetallic complex **1** (Figure 5). It crystallizes in the monoclinic system, space group  $P2_1/n$  with one dinuclear complex in the general position in the unit cell, organized into layers perpendicular to the *c* axis. Within one layer, the molecules are perpendicular to each other, now with the btt moiety systematically sandwiched between two  $\text{Cp}^*$  rings, with the shortest  $\text{C}_{\text{Cp}^*}\text{-C}_{\text{btt}}$  intermolecular distances 3.585(7) and 3.616(7) Å, indicating that the  $\text{Cp}^*$  and btt moieties are

(41) (a) Don, M.-J.; Yang, K.; Bott, S. G.; Richmond, M. G. *J. Organomet. Chem.* **1997**, *544*, 15. (b) Kawabata, K.; Nakano, M.; Tamura, H.; Matsubayashi, G. *J. Organomet. Chem.* **2004**, *689*, 405. (c) Nomura, M.; Fujii, M.; Fukuda, K.; Sugiyama, T.; Yokoyama, Y.; Kajitani, M. *J. Organomet. Chem.* **2005**, *690*, 1627.  
 (42) Miller, E. J.; Brill, T. B.; Rheingold, A. L.; Fultz, W. C. *J. Am. Chem. Soc.* **1983**, *105*, 7580.  
 (43) Mashima, K.; Kaneyoshi, H.; Kaneko, S.; Mikami, A.; Tani, K.; Nakamura, A. *Organometallics* **1997**, *16*, 1016.  
 (44) Xi, R.; Abe, M.; Suzuki, T.; Nishioka, T.; Isobe, K. *J. Organomet. Chem.* **1997**, *549*, 117.

(45) (a) Fourmigué, M.; Avarvari, N. *Dalton Trans.* **2005**, 1365. (b) Nomura, M.; Geoffroy, M.; Adkine, P.; Fourmigué, M. *Eur. J. Inorg. Chem.* **2006**, *5012*. (c) Nomura, M.; Fourmigué, M. *New J. Chem.* **2007**, *31*, 528.  
 (46) Perrocheau, V.; Fourmigué, M. *Acta Crystallogr.* **1997**, *C53*, 1213.  
 (47) Nomura, M.; Cauchy, T.; Geoffroy, M.; Adkine, P.; Fourmigué, M. *Inorg. Chem.* **2006**, *45*, 8194.  
 (48) Cauchy, T.; Ruiz, E.; Jeannin, O.; Nomura, M.; Fourmigué, M. *Chem.—Eur. J.* **2007**, *13*, 8858.  
 (49) Nomura, M.; Kajitani, M. *J. Organomet. Chem.* **2006**, *691*, 2691.

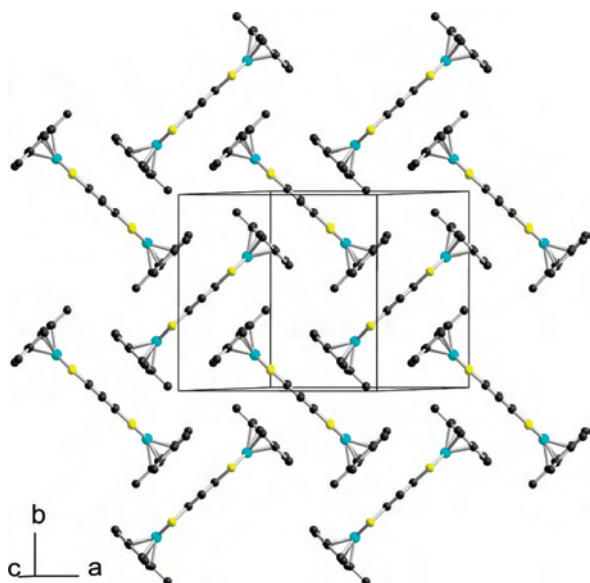


**Figure 5.** Projection view of one layer of the bimetallic molecules **1** showing the Cp\*–btt–Cp\* interactions, giving rise to a pseudo-4-fold-symmetry arrangement within the layers.

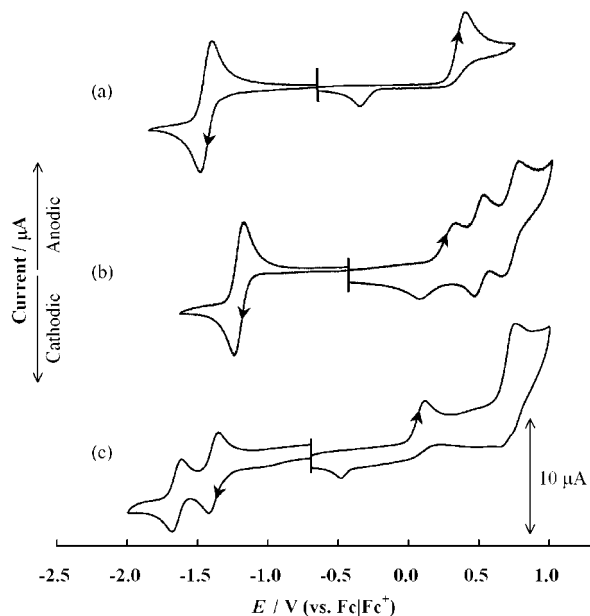


**Figure 6.** CVs of (a) **6**, (b) **8** ( $c = 1 \times 10^{-3} \text{ mol dm}^{-3}$ ), and (c) **1** ( $c = 5 \times 10^{-4} \text{ mol dm}^{-3}$ ) in a dichloromethane solution containing  $0.1 \text{ mol dm}^{-3}$   $\text{NBu}_4\text{PF}_6$  ( $\nu = 100 \text{ mV s}^{-1}$ ; working electrode  $1.0 \text{ mm}$  in diameter; Pt disk).

at van der Waals contact to afford this highly ordered compact structure, with a pseudo-4-fold-symmetry arrangement.

**Electrochemistry and Electronic Properties of Cp\*Co Dithiolene Complexes.** Cyclic voltammetry of the cobalt complexes were measured in a dichloromethane solution. Representative cyclic voltammograms (CVs) are shown in Figure 6, and the associated redox potentials (vs  $\text{Fc}/\text{Fc}^+$ ) are summarized in Table 2. The mononuclear complexes exhibit one well-defined reversible reduction wave at  $-1.40/-1.20 \text{ V}$  and one or several irreversible oxidation waves. The dinuclear complex **1** is characterized by two reversible reduction waves at  $-1.37$  and  $-1.63 \text{ V}$  and two

irreversible oxidation waves at  $+0.08$  and  $+0.71 \text{ V}$ . Because the reduction process in these complexes is associated with a  $\text{Co}^{\text{III}}$  to  $\text{Co}^{\text{II}}$  electron transfer, the two  $\text{Co}^{\text{III}}$  atoms in complex **1** are reduced stepwise to the  $\text{Co}^{\text{II}}$  species. The difference of two reduction potentials ( $\Delta E_{1/2}$ ) in complex **1** is equal to  $269 \text{ mV}$  (Table 2), suggesting the existence of a stable mixed-valence  $\text{Co}^{\text{III}}-\text{Co}^{\text{II}}$  state. Note also that this  $\Delta E_{1/2}$  value is larger or comparable to those observed in the dinuclear CpCo dithiolene complexes  $[\text{CpCo}(\text{S}_2\text{C}_2(\text{R}))_2]$  (**9**) shown in Chart 2 where the two metallacycles are linked through a single covalent bond ( $\Delta E_{1/2} = 160\text{--}222 \text{ mV}$  for  $\text{R} = \text{Me}, \text{Ph}, p\text{-C}_6\text{H}_4\text{COMe}, p\text{-C}_6\text{H}_4\text{NO}_2$ ;  $\Delta E_{1/2} = 262\text{--}285 \text{ mV}$  for  $\text{R} = \text{H}, \text{SiMe}_3$ ).<sup>20</sup> Comparison with the trinuclear cobaltadithiolene complex **10** is also interesting because it possesses a similar rigid coplanar benzene center. **10** was reported to reduce at  $-1.06, -1.30,$  and  $-1.74 \text{ V}$  (in THF), which affords a comparable, albeit slightly smaller  $\Delta E_{1/2}$  between the two first reduction waves ( $240 \text{ mV}$ ). Note also that a much larger  $\Delta E_{1/2}$  value ( $650\text{--}660 \text{ mV}$ ) was reported in the dinuclear Cp\*Co dithiolene complex with the  $\text{tto}^{4-}$  ligand  $[\text{Cp}^*\text{Co}(\text{tto})\text{CoCp}^*]$  (Chart 1), as a consequence of the closer proximity of the two Co metal centers with the smaller  $\text{tto}$  ligand, when compared with the  $\text{btt}$  ligand investigated here.<sup>19</sup>

The UV–vis spectral data of Cp\*Co dithiolene complexes are summarized in Table 3. All complexes exhibit a broad absorption band in the visible range, between  $575$  and  $675 \text{ nm}$ . The bimetallic complex **1** exhibits a  $103 \text{ nm}$  red shift compared with the unsubstituted **6** complex, while its absorption compares with that of the  $\text{dmit}$  derivative **8**. Note also the very large molar absorption coefficient value ( $\epsilon = 31\,000 \text{ M}^{-1}\text{cm}^{-1}$ ) of **1** compared with the other mononuclear  $[\text{Cp}^*\text{Co}(\text{dithiolene})]$  complexes ( $\epsilon = 8600\text{--}12\,000 \text{ M}^{-1}\text{cm}^{-1}$ ).

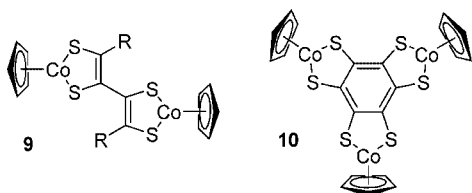
**Formation of  $\text{P}(\text{OMe})_3$  Adducts and Their Molecular Structures.** Henderson, Kajitani, and co-workers have reported that phosphines and phosphites react readily with CpCo(dithiolene) to afford the corresponding 1:1 adducts,  $[\text{CpCo}(\text{dithiolene})(\text{PR}_3)]$ .<sup>26</sup> However, the corresponding adducts with the Cp\* complexes have been barely explored so far. Indeed, only the cationic  $[\text{Cp}^*\text{Co}(\text{dddt})(\text{P}(\text{OMe})_3)]^+$  ( $\text{dddt} = 5,6\text{-dihydro-1,4-dithione-2,3-dithiolate}$ ) and dicationic  $[\text{Cp}^*\text{Co}(\text{tto})\text{CoCp}^*(\text{P}(\text{OMe})_3)_2]^{2+}$  species are known,<sup>19,50</sup> while the corresponding neutral species have not been described so far. The reaction of **8** with 10 equiv of  $\text{P}(\text{OMe})_3$  in a dichloromethane solution leads to a rapid color change from green to dark red. The  $\text{P}(\text{OMe})_3$  adduct of complex **8** is precipitated in quantitative yield by the slow addition of pentane. Similarly, the bimetallic complex **1** reacted immediately in the presence of a large excess of  $\text{P}(\text{OMe})_3$  in a chloroform solution to afford a brown product. Note, however, that the phosphite coordination is reversible because, upon dissolution of these isolated  $\text{P}(\text{OMe})_3$  adducts in an organic solvent, the phosphite is eliminated to regenerate the original complexes **1** and **8**, respectively. The coordinating  $\text{P}(\text{OMe})_3$  is also eliminated quantitatively if a

(50) Guyon, F.; Lucas, D.; Jourdain, I. V.; Fourmigué, M.; Mugnier, Y.; Catey, H. *Organometallics* **2001**, *20*, 2421.

**Table 2.** Redox Potentials (in V vs Fc/Fc<sup>+</sup>) of Cp\*Co and CpCo Dithiolene Complexes

compound	solvent	$E_{1/2}^{\text{red}2}$	$E_{1/2}^{\text{red}2}$	$E_{1/2}^{\text{ax}1}$	$E_{1/2}^{\text{ax}2}$	$E_{1/2}^{\text{ax}3}$	ref
<b>1</b>	CH <sub>2</sub> Cl <sub>2</sub>	-1.37	-1.63	+0.08 <sup>a</sup>	+0.71 <sup>a</sup>	<i>b</i>	this work
[Cp*Co(tto)CoCp*]	CH <sub>2</sub> Cl <sub>2</sub>	-0.90	-1.56	0.51 <sup>a</sup>	<i>c</i>	<i>c</i>	19
[CpCo(S <sub>2</sub> C <sub>2</sub> (H)) <sub>2</sub> ]	CH <sub>2</sub> Cl <sub>2</sub>	-0.67	-0.950	<i>c</i>	<i>c</i>	<i>c</i>	20
<b>4a</b>	CH <sub>2</sub> Cl <sub>2</sub>	-1.38	<i>b</i>	+0.34 <sup>a</sup>	<i>b</i>	<i>b</i>	this work
<b>4b</b>	CH <sub>2</sub> Cl <sub>2</sub>	-1.34	<i>b</i>	+0.44 <sup>a</sup>	+0.65 <sup>a</sup>	<i>b</i>	this work
<b>4c</b>	CH <sub>2</sub> Cl <sub>2</sub>	-1.44	<i>b</i>	+0.26 <sup>a</sup>	<i>b</i>	<i>b</i>	this work
[Cp*Co(bdt)] ( <b>6</b> )	CH <sub>2</sub> Cl <sub>2</sub>	-1.44	<i>b</i>	+0.37 <sup>a</sup>	<i>b</i>	<i>b</i>	this work
[Cp*Co(dmit)] ( <b>8</b> )	CH <sub>2</sub> Cl <sub>2</sub>	-1.21	<i>b</i>	+0.20 <sup>a</sup>	+0.50	+0.74	this work
[ <b>1</b> -P(OMe) <sub>3</sub> ]	CH <sub>2</sub> Cl <sub>2</sub>	-1.57 <sup>a</sup>	<i>b</i>	-0.41 <sup>a</sup>	-0.17	+0.79	this work
[ <b>8</b> -P(OMe) <sub>3</sub> ]	CH <sub>2</sub> Cl <sub>2</sub>	-1.62 <sup>a</sup>	<i>b</i>	-0.18	+0.55	+0.65	this work

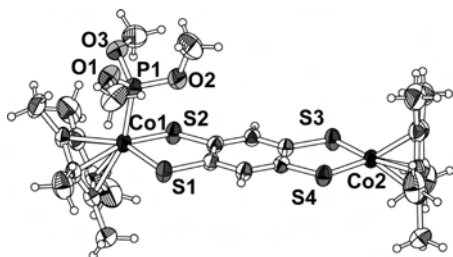
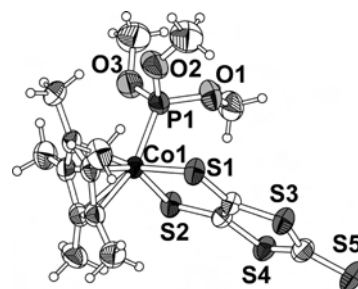
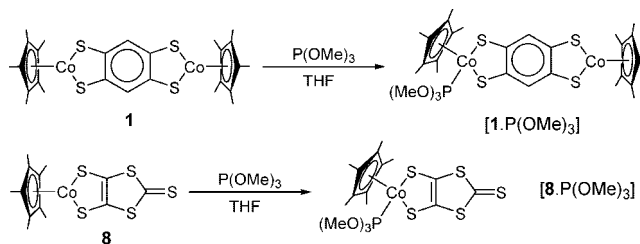
<sup>a</sup> Irreversible. <sup>b</sup> Not found. <sup>c</sup> Not available.

**Chart 2****Table 3.** UV-Vis Spectral Data of Cp\*Co Dithiolene Complexes

complex	solvent	$\lambda_{\text{max}}/\text{nm}$	$\epsilon/\text{M}^{-1}\text{cm}^{-1}$
<b>1</b>	CH <sub>2</sub> Cl <sub>2</sub>	677	31 000
<b>4a</b>	CH <sub>2</sub> Cl <sub>2</sub>	613	10 000
<b>4b</b>	CH <sub>2</sub> Cl <sub>2</sub>	585	11 000
<b>4c</b>	CH <sub>2</sub> Cl <sub>2</sub>	637	10 000
<b>6</b>	CH <sub>2</sub> Cl <sub>2</sub>	574	8 600
<b>8</b>	CH <sub>2</sub> Cl <sub>2</sub>	677	12 000

solution of the adduct is subjected to column chromatography on silica gel. These observations suggest that the phosphite association constants are relatively small. Also, the bimetallic complex **1** is susceptible to association with either one or two phosphite molecules, with probably different association constants. These points have been addressed below based on a combination of mass spectroscopy, <sup>1</sup>H NMR, and optical spectroscopic methods.

The product of the reaction of complex **8** with P(OMe)<sub>3</sub> was identified as the 1:1 adduct [Cp\*Co(dmit)(P(OMe)<sub>3</sub>)] [**8**-P(OMe)<sub>3</sub>], on the basis of its mass spectrum and elemental analysis (Scheme 4). The <sup>1</sup>H NMR spectra of these P(OMe)<sub>3</sub> adducts were obtained from CDCl<sub>3</sub> solutions of complexes **1** and **8** in the presence of 1000 equiv of P(OMe)<sub>3</sub>. In the complex [**8**-P(OMe)<sub>3</sub>], there are two doublet signals: one doublet at 3.87 ppm ( $J_{\text{P-H}} = 9.7$  Hz) for the OMe groups of P(OMe)<sub>3</sub> and another at 1.51 ppm ( $J_{\text{P-H}} = 2.7$  Hz) for the Me groups of the Cp\* ligand. The P(OMe)<sub>3</sub> adduct of complex **1** gave, for the Me groups of the two Cp\* rings, a doublet at 1.52 ppm (15H,  $J_{\text{P-H}} = 2.6$  Hz) and a singlet signal

**Figure 7.** ORTEP drawing of [**1**-P(OMe)<sub>3</sub>]. The thermal ellipsoids are drawn at the 50% probability level.**Figure 8.** ORTEP drawing of [**8**-P(OMe)<sub>3</sub>]. The thermal ellipsoids are drawn at the 50% probability level.**Scheme 4****Table 4.** Selected Bond Lengths (Å) and Angles (deg) in P(OMe)<sub>3</sub> Adducts

complex	[ <b>1</b> -P(OMe) <sub>3</sub> ]		
	[ <b>8</b> -P(OMe) <sub>3</sub> ]	Co1 side	Co2 side
Bond Length			
Co1-S1 (Co2-S3)	2.2553(7)	2.2313(9)	2.1250(9)
Co1-S2 (Co2-S4)	2.2586(7)	2.2292(8)	2.1294(9)
S1-C1 (S3-C4)	1.733(2)	1.755(3)	1.739(3)
S2-C2 (S4-C5)	1.742(3)	1.760(3)	1.745(3)
C1-C2	1.352(4)	1.402(4)	
C2-S3		1.389(4)	
C3-C4		1.411(4)	
C4-C5		1.401(4)	
C5-C6		1.400(4)	
C1-C6		1.393(4)	
Bond Angle			
S1-Co1-S2 (S3-Co2-S4)	92.88(2)	90.15(3)	92.21(3)
Co1-S1-C1 (Co2-S3-C4)	100.07(9)	104.15(11)	105.40(11)
Co1-S2-C2 (Co2-S4-C5)	99.84(8)	104.29(10)	105.27(10)
S1-C1-C2 (S3-C4-C5)	123.64(19)	120.2(2)	118.8(2)
S2-C2-C1 (S4-C5-C4)	123.41(18)	119.7(2)	118.4(2)
Cp*/dithiolene dihedral angle	52.87	52.75	88.53
dithiolene mean plane deviation	0.0239	0.0751	0.0032

at 2.00 ppm (15H), indicating unambiguously that, under these conditions, only one phosphite molecule is coordinated to the bimetallic complex, despite the presence of two Co centers. Apparently, the coordinated P(OMe)<sub>3</sub> increases the electron density on the other P(OMe)<sub>3</sub>-free Co atom through an electronic conjugation of the central btt<sup>4-</sup> ligand, thus

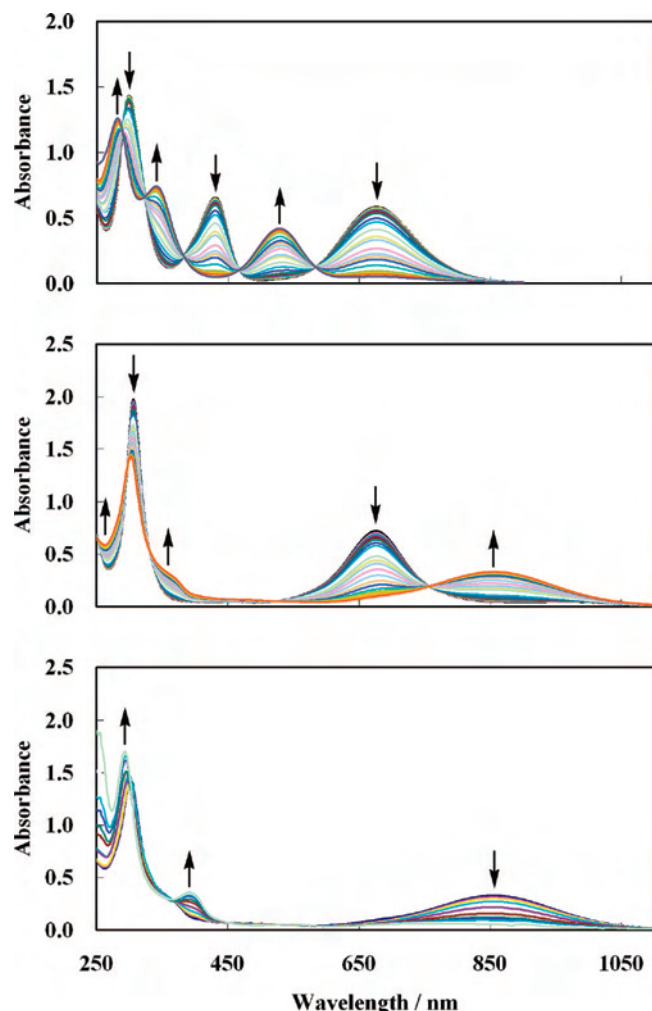


**Figure 9.** UV-vis-NIR spectral changes of (top) complex **8** ( $c = 5.0 \times 10^{-5} \text{ mol}\cdot\text{dm}^{-3}$ ) by the addition of  $\text{P}(\text{OMe})_3$  ( $0\text{--}10^3$  equiv), (middle) complex **1** ( $c = 2.5 \times 10^{-5} \text{ mol}\cdot\text{dm}^{-3}$ ) by the addition of  $\text{P}(\text{OMe})_3$  ( $0\text{--}10^3$  equiv), and (bottom) complex **1** by the addition of  $\text{P}(\text{OMe})_3$  ( $10^3\text{--}10^5$  equiv) in a dichloromethane solution.

deactivating the Lewis acid character of the second Co center. The mass spectrum and elemental analysis supported the structure of a 1:1 adduct shown in Scheme 4,  $[\text{Cp}^*\text{Co}(\text{btt})\text{CoCp}^*(\text{P}(\text{OMe})_3)]$ ,  $[\mathbf{1}\cdot\text{P}(\text{OMe})_3]$ .

The molecular structures of both monophosphite adducts,  $[\mathbf{1}\cdot\text{P}(\text{OMe})_3]$  and  $[\mathbf{8}\cdot\text{P}(\text{OMe})_3]$ , were obtained from single-crystal X-ray diffraction data (Figures 7 and 8), and selected bond lengths and angles are reported in Table 4. These complexes adopt a three-legged piano-stool structure through the coordination of  $\text{P}(\text{OMe})_3$  to the Co atom. The dihedral angles between the  $\text{Cp}^*$  and  $\text{CoS}_2$  mean planes amount to  $52.75^\circ$  and  $52.87^\circ$  for  $[\mathbf{1}\cdot\text{P}(\text{OMe})_3]$  and  $[\mathbf{8}\cdot\text{P}(\text{OMe})_3]$ , respectively. In complex  $[\mathbf{1}\cdot\text{P}(\text{OMe})_3]$ , because the  $\text{P}(\text{OMe})_3$ -free Co atom is coordinatively unsaturated, the dihedral angle between the  $\text{Cp}^*$  and  $\text{CoS}_2$  mean planes still amounts to  $90^\circ$ .

The changes in the UV-vis-NIR spectra of the dinuclear complex **1** and the mononuclear complex **8** upon the addition of  $\text{P}(\text{OMe})_3$  are shown in Figure 9. For the complex **8**, the absorption maximum at 677 nm decreases while a new absorption appears at 529 nm ( $\epsilon = 8400 \text{ M}^{-1}\cdot\text{cm}^{-1}$ ; Table

5), attributed to the formation of the  $[\mathbf{8}\cdot\text{P}(\text{OMe})_3]$  adduct. The spectral change was complete only after the addition of 1000 equiv of  $\text{P}(\text{OMe})_3$ . Such a blue shift has been reported for  $[\text{CpCo}(\text{dithiolene})]$  complexes.<sup>26b</sup> In the dinuclear complex **1**, the absorption band at 677 nm also decreased in intensity upon  $\text{P}(\text{OMe})_3$  addition ( $0\text{--}10^3$  equiv), but interestingly, a new absorption band appeared in the NIR region with  $\lambda_{\text{max}} = 856 \text{ nm}$  ( $\epsilon = 13\,000 \text{ M}^{-1}\cdot\text{cm}^{-1}$ ; Figure 10, middle, and Table 5). Furthermore, this NIR absorption band decreases in intensity when more than  $10^3$  equiv of  $\text{P}(\text{OMe})_3$  was added (Figure 10, bottom). These results suggest the sequential formation of the mono- $\text{P}(\text{OMe})_3$  and bis- $\text{P}(\text{OMe})_3$  adducts, while the low-energy absorption band of the monophosphite adduct is attributable to a lowering of the HOMO-LUMO gap when going from **1** to  $[\mathbf{1}\cdot\text{P}(\text{OMe})_3]$ .

The corresponding formation constants (concentration basis) of these  $\text{P}(\text{OMe})_3$  adducts are defined by

$$K = [\text{YL}]/[\text{Y}][\text{L}] \quad (1)$$

where  $[\text{L}]$  is the concentration of the unbound ligand  $\text{P}(\text{OMe})_3$ ,  $[\text{Y}]$  that of the unbound  $[\text{CpCo}(\text{dithiolene})]$ , and  $[\text{YL}]$  that of the adduct. The value of  $K$  was determined according to eq 2.

$$(A_0 - A)/(A - A^*) = K[c_L - c(A_0 - A)/(A_0 - A^*)] \quad (2)$$

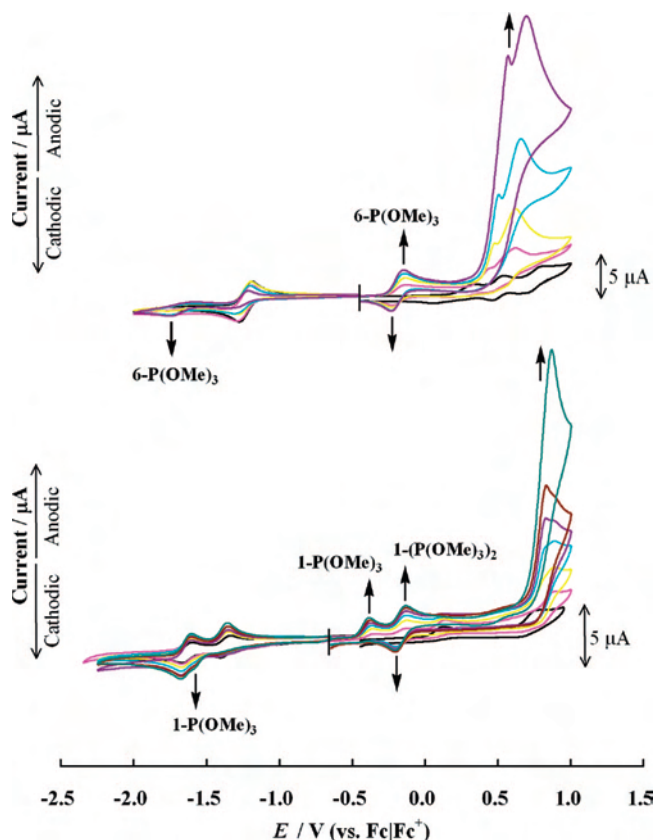
where  $A$  is the absorbance of the mixture containing  $\text{L}$  and the complex at total concentrations  $c_L$  and  $c$ , respectively,  $A_0$  is the absorbance of a solution containing only the complex at  $c$ , and  $A^*$  is the absorbance of the solution containing only the adduct at concentration  $c$ .<sup>26b</sup> Experimentally,  $A^*$  can be estimated from the absorbance of a solution containing a sufficiently large excess of  $\text{L}$ . When the left-hand side of eq 2 is plotted against the quantity in the square brackets on the right-hand side, a straight line passing the origin should result, the slope of which gives  $K$ .

The formation constants ( $K$ ) of several  $\text{P}(\text{OMe})_3$  adducts have been determined here for complexes **1**, **4b**, **6**, and **8** from the evolution of their UV-vis-NIR spectra in the presence of various concentrations of  $\text{P}(\text{OMe})_3$  (Table 5). The experimental  $K$  values determined here for the  $\text{Cp}^*$  complexes are comparable to those described for  $\text{Cp}$  complexes, indicating that the permethylation of the  $\text{Cp}$  ring has a small effect on the Lewis acid character of the Co center. In the  $\text{Cp}^*$  series, we also observe that the bimetallic complex **1** and the dmit derivative **8**,  $[\text{Cp}^*\text{Co}(\text{dmit})]$ , present the strongest affinity for phosphite coordination, in accordance with their most negative reduction potentials. Indeed, Kajitani et al. have reported a linear correlation between  $K$  and the reduction potential of the  $\text{PR}_3$ -free  $[\text{CpCo}(\text{dithiolene})]$  complexes.<sup>26b</sup>

**Electrochemistry of  $\text{P}(\text{OMe})_3$  Adducts.** Upon the sequential addition of increasing amounts of  $\text{P}(\text{OMe})_3$ , the CVs of the dinuclear complex **1** and mononuclear complex **8** are strongly modified, as displayed in Figure 10. Indeed, the first reduction wave of complex **8** at  $-1.21 \text{ V}$  decreases in intensity upon the addition of  $\text{P}(\text{OMe})_3$ , while a new irreversible reduction wave appears at  $-1.62 \text{ V}$  (Table 2). Three oxidation waves in the original complex **8** disappear,

**Table 5.** UV–Vis–NIR Data and Logarithm of Formation Constants,  $\log(K)/\text{mol}^{-1}\cdot\text{dm}^3$ , of the  $\text{P}(\text{OMe})_3$  Adducts of CpCo and Cp\*Co Dithiolene Complexes

	solvent	$\log(K)/\text{mol}^{-1}\cdot\text{dm}^3$	$\lambda_{\text{max}}/\text{nm}$	$\epsilon/\text{M}^{-1}\cdot\text{cm}^{-1}$	ref
[ <b>1</b> · $\text{P}(\text{OMe})_3$ ]	$\text{CH}_2\text{Cl}_2$	3.1	856	13000	this work
[ <b>1</b> · $\text{P}(\text{OMe})_3$ ] <sub>2</sub>	$\text{CH}_2\text{Cl}_2$	0.52			this work
[ <b>4b</b> · $\text{P}(\text{OMe})_3$ ]	$\text{CH}_2\text{Cl}_2$	2.0	377	9000	this work
[ <b>6</b> · $\text{P}(\text{OMe})_3$ ]	$\text{CH}_2\text{Cl}_2$	2.0	351	7500	this work
[ <b>8</b> · $\text{P}(\text{OMe})_3$ ]	$\text{CH}_2\text{Cl}_2$	2.8	529	8400	this work
[CpCo(mnt)( $\text{P}(\text{OMe})_3$ )]	MeCN	5.3			26b
[CpCo( $\text{S}_2\text{C}_2(\text{COOMe})_2$ )( $\text{P}(\text{OMe})_3$ )]	MeCN	2.9			26b
[CpCo( $\text{S}_2\text{C}_2\text{Py}_2$ )( $\text{P}(\text{OMe})_3$ )]	MeCN	1.7			26b
[CpCo( $\text{S}_2\text{C}_2\text{Ph}_2$ )( $\text{P}(\text{OMe})_3$ )]	MeCN	0.55			26b

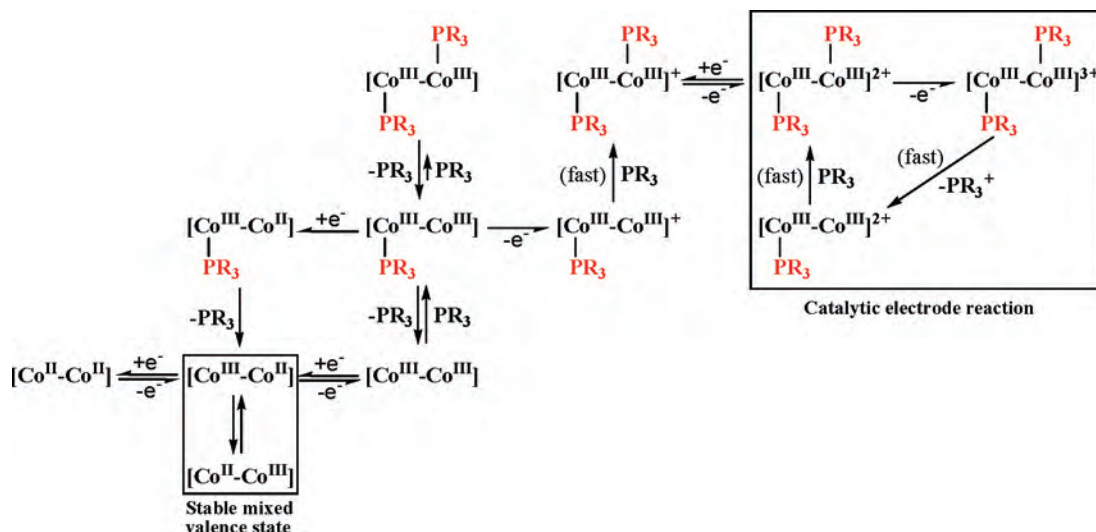
**Figure 10.** CV changes of (bottom) complex **1** ( $c = 5 \times 10^{-4} \text{ mol}\cdot\text{dm}^{-3}$ ) by the addition of  $\text{P}(\text{OMe})_3$  (0–10 equiv) and (top) complex **8** ( $c = 1 \times 10^{-3} \text{ mol}\cdot\text{dm}^{-3}$ ) by the addition of  $\text{P}(\text{OMe})_3$  (0–10 equiv) in a dichloromethane solution containing  $0.1 \text{ mol}\cdot\text{dm}^{-3}$   $\text{NBu}_4\text{PF}_6$  ( $\nu = 100 \text{ mV}\cdot\text{s}^{-1}$ ; working electrode 1.0 mm in diameter; Pt disk).

while a new, reversible oxidation wave at  $-0.18 \text{ V}$  and two irreversible oxidation waves appeared around  $+0.55$  to  $+0.65 \text{ V}$  (Table 2). Note that the anodic current of oxidation waves exhibits a strong increase upon  $\text{P}(\text{OMe})_3$  addition. Similarly, in the bimetallic complex **1**, the first reversible reduction wave at  $-1.37 \text{ V}$  decreases upon  $\text{P}(\text{OMe})_3$  addition with the concomitant apparition of a new, irreversible reduction wave at  $-1.57 \text{ V}$ . The second reduction wave ( $-1.63 \text{ V}$ ) of the original complex **1** does not change and its reversibility is maintained. There are three new oxidation waves at  $-0.41 \text{ V}$  (irreversible),  $-0.17 \text{ V}$  (reversible), and  $+0.79 \text{ V}$  (irreversible). Again, the anodic current of the third oxidation wave remarkably changed depending on the amount of  $\text{P}(\text{OMe})_3$ .

We first observe that  $\text{P}(\text{OMe})_3$  coordination induces a cathodic shift of the reduction potentials of the cobalt

complexes because it increases the electron density at the Co. This shift in the first reduction wave amounts to  $-0.41 \text{ V}$  in **8** but only  $-0.20 \text{ V}$  in the dinuclear complex **1**. Indeed, in the latter, the first reduction potential is most probably associated with the  $\text{P}(\text{OMe})_3$ -free, coordinatively unsaturated Co atom. Phosphite coordination of the other Co atom influences, however to some extent, the noncoordinated one, demonstrating that there is a metal–metal electronic interaction through the conjugating  $\text{btt}^{4-}$  ligand. Because the reduction waves of [**1**· $\text{P}(\text{OMe})_3$ ] and [**8**· $\text{P}(\text{OMe})_3$ ] are irreversible, a chemical reaction following the reduction has to be considered (EC reaction). On the basis of earlier reports on phosphine complexes [CpCo(dithiolene)( $\text{PR}_3$ )],<sup>26b</sup> we can assume that the coordinated  $\text{P}(\text{OMe})_3$  is eliminated upon reduction (Scheme 5). The reversible oxidation of [**8**· $\text{P}(\text{OMe})_3$ ] demonstrates that the monocation species [**8**· $\text{P}(\text{OMe})_3$ ]<sup>+</sup> is stable on the time scale of CV ( $\nu = 100 \text{ mV}\cdot\text{s}^{-1}$ ), in accordance with previous reports on the stability of [CpCo(dithiolene)( $\text{PR}_3$ )]<sup>+</sup> monocationic complexes.<sup>50,51</sup> On the other hand, the irreversible wave observed during the oxidation of [**1**· $\text{P}(\text{OMe})_3$ ] (Figure 10) seems to contradict this assumption. This irreversible character is most probably associated with the coordination of a second phosphite molecule on the cationic [**1**· $\text{P}(\text{OMe})_3$ ]<sup>+</sup> species to afford the monocationic bisadduct [**1**· $\text{P}(\text{OMe})_3$ ]<sub>2</sub><sup>+</sup>, which then displays a reversible oxidation process at  $-0.17 \text{ V}$  to generate the corresponding [**1**· $\text{P}(\text{OMe})_3$ ]<sub>2</sub><sup>2+</sup> dication. A similar dicationic complex [Cp\*Co(tto)CoCp\*( $\text{P}(\text{OMe})_3$ )<sub>2</sub>]<sup>2+</sup> was isolated from the reaction of [Cp\*Co(tto)CoCp\*] with  $\text{P}(\text{OMe})_3$  in the presence of a chemical oxidant.<sup>19</sup> At the higher anodic potentials, a current much bigger than the usual oxidation current is observed on the CVs of both **1** and **8**, demonstrating that a catalytic reaction on the electrode is taking place (Figure 10). This oxidation wave is related to the electrochemical oxidation of the monocationic [**8**· $\text{P}(\text{OMe})_3$ ]<sup>+</sup> to the dicationic [**8**· $\text{P}(\text{OMe})_3$ ]<sub>2</sub><sup>2+</sup>. At this stage, the following reaction mechanism can be considered, as is also shown in the right part of Scheme 5: (1) the elimination of radical cation  $\text{P}(\text{OMe})_3^{+\cdot}$  from dication [**8**· $\text{P}(\text{OMe})_3$ ]<sub>2</sub><sup>2+</sup> to generate monocation **8**<sup>+</sup>, (2) the fast addition of  $\text{P}(\text{OMe})_3$  present in excess to **8**<sup>+</sup> to regenerate the monocation [**8**· $\text{P}(\text{OMe})_3$ ]<sup>+</sup>, (3) the reoxidation of the monocation [**8**· $\text{P}(\text{OMe})_3$ ]<sup>+</sup> to dication [**8**· $\text{P}(\text{OMe})_3$ ]<sub>2</sub><sup>2+</sup>, and (4) the reaction (1) occurs again. A similar catalytic reaction was already identified in [CpCo(dithiolene)(L)] (L = MeCN,  $\text{PR}_3$ ).<sup>51</sup>

Interestingly, typical tertiary phosphites are not oxidized at low potentials, at least not oxidized in the potential window

Scheme 5. Summary of Electrochemical (E) and Chemical (C) Reactions of Complexes **1** and  $[\mathbf{1}\cdot\text{P}(\text{OMe})_3]^a$ 

<sup>a</sup> The E reactions are toward the right and left. The C reactions are toward up and down.

of  $\text{CH}_2\text{Cl}_2/\text{NBu}_4\text{PF}_6$ . Therefore, the catalytic reaction identified here can efficiently generate the phosphite radical cation without the need for high oxidation potentials. Such tertiary phosphorus radical compounds can be used for the efficient synthesis of a phosphonium salt.<sup>52</sup> In addition, the electron-rich  $\text{Cp}^*\text{Co}$  complex,  $[\text{Cp}^*\text{Co}(\text{dithiolene})(\text{L})]$ , can be oxidized at a lower oxidation potential than that in the case of the Cp derivatives  $[\text{CpCo}(\text{dithiolene})(\text{L})]$ . A very similar behavior is also identified in the CV of the bimetallic complex  $[\mathbf{1}\cdot\text{P}(\text{OMe})_3]$  (Figure 10). The third oxidation wave that exhibits this strong current enhancement is therefore associated with the oxidation of the dication  $[\mathbf{1}\cdot\text{P}(\text{OMe})_3]^{2+}$  to the trication  $[\mathbf{1}\cdot\text{P}(\text{OMe})_3]^{3+}$ . At this stage, the elimination of radical  $\text{P}(\text{OMe})_3^{\cdot+}$ , the addition of  $\text{P}(\text{OMe})_3$ , and the reoxidation of the dicationic  $\text{P}(\text{OMe})_3$  adduct are also cyclically repeated (Scheme 5).

## Conclusion

We have shown here that the bis(dibutyltin) derivative **5** was a very attractive intermediate for the preparation of bimetallic complexes such as **1**. These  $\text{Cp}^*\text{Co}$  derivatives of benzenetetrathiolate or benzenedithiolate exhibit a recurrent structural motif with a parallel  $\text{Cp}^*$  and btt (or bdt) arrangement, stabilizing the formation of 4-fold-symmetry motifs. The two reduction steps of the bimetallic complex **1** are associated with the sequential  $\text{Co}^{\text{III}}\text{--Co}^{\text{II}}$  processes with a  $\Delta E_{1/2}$  value of 0.27 V, demonstrating a sizable interaction between both metal centers. This is also confirmed by the stability constants for phosphite association, determined from spectroscopic titration experiments at 3.1 and 0.5  $\text{mol}^{-1}\cdot\text{dm}^3$  for the mono- and bis-phosphite adducts, respectively. Phosphite coordination is also associated with a strong red

shift of the low-energy absorption band, observed at 677 nm in complex **1** but in the NIR at 856 nm in  $[\mathbf{1}\cdot\text{P}(\text{OMe})_3]$ . The relatively weak affinity for phosphite is strongly enhanced upon oxidation because, for example, the radical  $[\mathbf{1}\cdot\text{P}(\text{OMe})_3]^{\cdot+}$  species rapidly adds a second  $\text{P}(\text{OMe})_3$  molecule upon oxidation to form the stable dicationic bisadduct  $[\mathbf{1}\cdot\text{P}(\text{OMe})_3]^{2+}$ . Further oxidation leads to a catalytic cycle to generate the radical  $[\text{P}(\text{OMe})_3]^{\cdot+}$  cation.

## Experimental Section

**General Remarks.** All reactions were carried out under an argon atmosphere by means of standard Schlenk techniques. All solvents for chemical reactions were dried and distilled by sodium benzophenone (for toluene) or by  $\text{CaH}_2$  (for methanol) before use. Trimethyl phosphite was obtained from Aldrich.  $[\text{Cp}^*\text{Co}(\text{CO})\text{I}_2]$ ,<sup>53</sup> **2**,<sup>54</sup> **3**,<sup>55,56</sup> and **7**<sup>57</sup> were prepared by literature methods. Silica gel (silica gel 60) was obtained from Merck, Ltd. Melting points were measured on a Kofler hot-stage apparatus and are uncorrected. <sup>1</sup>H NMR spectra were recorded on a Bruker ARX 200 spectrometer. Chemical shifts are quoted in parts per million (ppm) and referenced to tetramethylsilane (TMS). Mass spectra were recorded with a Varian MAT 311 instrument by the Centre Régional de Mesures Physiques de l'Ouest, Rennes, France. Elemental analyses were performed at the Laboratoire Central de Microanalyse du CNRS, Lyon, France. UV-vis and NIR spectra were recorded on a Shimadzu model UV-1605 spectrophotometer.

**Reaction of  $[\text{Cp}^*\text{Co}(\text{CO})\text{I}_2]$  with **2**.** 1,2,4,5-Tetrakis(isopropylthio)benzene (**2**) (187 mg, 0.5 mmol) was reacted with sodium (69 mg, 3.0 mmol) in dry pyridine (10 mL) for 1.5 h at 100 °C. A dark-red solution was obtained. The solution was cooled down to room temperature. A THF solution (30 mL) of  $[\text{Cp}^*\text{Co}(\text{CO})\text{I}_2]$  (476 mg, 1.0 mmol) was added. The reaction mixture was further stirred

- (51) Shimizu, K.; Ikehara, H.; Kajitani, M.; Ushijima, H.; Akiyama, T.; Sugimori, A.; Satô, G. P. *J. Electroanal. Chem.* **1995**, *396*, 465.  
 (52) (a) Maeda, H.; Ohmori, H. *Acc. Chem. Res.* **1999**, *32*, 72. (b) Ohmori, H.; Takanami, T.; Masui, M. *Tetrahedron Lett.* **1985**, *26*, 2199. (c) Maeda, H.; Koide, T.; Maki, T.; Ohmori, H. *Chem. Pharm. Bull.* **1995**, *43*, 1076.

- (53) Frith, S. A.; Spencer, J. L. *Inorg. Synth.* **1985**, *23*, 15.  
 (54) Dirk, C. W.; Cox, S. D.; Wellman, D. E.; Wudl, F. *J. Org. Chem.* **1985**, *50*, 2395.  
 (55) Lange, S. J.; Nie, H.; Stern, C. L.; Barrett, A. G. M.; Hoffman, B. M. *Inorg. Chem.* **1998**, *37*, 6435.  
 (56) Larsen, J.; Bechgaard, K. *J. Org. Chem.* **1987**, *52*, 3285.  
 (57) De Mayo, P.; Weedon, A. C.; Wong, G. S. K. *J. Org. Chem.* **1979**, *44*, 1977.

Table 6. Crystallographic Data

compound	<b>1</b>	<b>4a</b>	<b>6</b>	[ <b>1</b> ·P(OMe) <sub>3</sub> ]	[ <b>8</b> ·P(OMe) <sub>3</sub> ]
formula	C <sub>26</sub> H <sub>32</sub> Co <sub>2</sub> S <sub>4</sub>	C <sub>22</sub> H <sub>31</sub> CoS <sub>4</sub>	C <sub>16</sub> H <sub>19</sub> CoS <sub>2</sub>	C <sub>29</sub> H <sub>41</sub> Co <sub>2</sub> O <sub>3</sub> PS <sub>4</sub>	C <sub>16</sub> H <sub>24</sub> CoO <sub>3</sub> PS <sub>5</sub>
fw (g·mol <sup>-1</sup> )	590.62	482.64	334.36	714.69	514.55
cryst color	blue	dark blue	purple	brown	brown
cryst shape	prism	prism	prism	block	prism
cryst size (mm)	0.12 × 0.08 × 0.05	0.22 × 0.17 × 0.06	0.42 × 0.32 × 0.202	0.50 × 0.40 × 0.22	0.29 × 0.22 × 0.055
cryst syst	monoclinic	monoclinic	orthorhombic	orthorhombic	triclinic
space group	<i>P</i> 2 <sub>1</sub> / <i>n</i>	<i>P</i> 2 <sub>1</sub> / <i>c</i>	<i>P</i> 2 <sub>1</sub> 2 <sub>1</sub> 2 <sub>1</sub>	<i>P</i> 2 <sub>1</sub> 2 <sub>1</sub> 2 <sub>1</sub>	<i>P</i> $\bar{1}$
<i>T</i> (K)	100	100	100	293	293
<i>a</i> (Å)	13.4903(6)	14.341(4)	8.1353(ç)	11.56020(10)	8.2864(2)
<i>b</i> (Å)	13.3205(7)	17.836(4)	13.5274(14)	15.0512(2)	11.2803(3)
<i>c</i> (Å)	15.9026(7)	18.804(5)	13.6835(14)	18.6825(2)	12.3231(3)
$\alpha$ (deg)	90.0	90.0	90.0	90.0	99.749(2)
$\beta$ (deg)	112.959(2)	96.203(12)	90.0	90.0	97.378(2)
$\gamma$ (deg)	90.0	90.0	90.0	90.0	93.5710(10)
<i>V</i> (Å <sup>3</sup> )	2631.3(2)	4782(2)	1505.9(3)	3250.66(6)	1121.68(5)
<i>Z</i>	4	8	4	4	2
<i>D</i> <sub>calc</sub> (g·cm <sup>-3</sup> )	1.491	1.341	1.475	1.460	1.523
$\mu$ (mm <sup>-1</sup> )	1.591	1.073	1.40	1.355	1.315
total reflns	28293	82881	14345	29706	9505
abs corr	multiscan	multiscan	multiscan	multiscan	multiscan
unique reflns ( <i>R</i> <sub>int</sub> )	6038 (0.0886)	10945 (0.0885)	3465 (0.0386)	7433 (0.0239)	5129 (0.0188)
unique reflns [ <i>I</i> > 2 $\sigma$ ( <i>I</i> )]	3407	9722	3341	6965	4290
<i>R</i> <sub>1</sub> , w <i>R</i> <sub>2</sub> [ <i>I</i> > 2 $\sigma$ ( <i>I</i> )] <sup>a</sup>	0.0547, 0.1433	0.0654, 0.1076	0.0206, 0.485	0.0422, 0.1110	0.0394, 0.1053
<i>R</i> <sub>1</sub> , w <i>R</i> <sub>2</sub> (all data) <sup>a</sup>	0.1240, 0.1778	0.0775, 0.1119	0.0221, 0.0494	0.0457, 0.1165	0.0486, 0.1133
GOF	1.034	1.238	1.028	1.156	1.069

$$^a R_1 = \sum ||F_o| - |F_c|| / \sum |F_o|; wR_2 = [\sum w(F_o^2 - F_c^2)^2 / \sum wF_o^4]^{1/2}.$$

for 2 h. Solvents (THF and pyridine) were removed under reduced pressure. The residue was separated by column chromatography on silica gel. Elution with dichloromethane/petroleum ether [2:1 (v/v)] afforded a blue fraction of **4a** in 29% yield after recrystallization from EtOH, while elution with dichloromethane afforded **1** in 33% yield after recrystallization from CHCl<sub>3</sub>/EtOH.

**1**. MS (FAB<sup>+</sup>): 590 ([M<sup>+</sup>]). HRMS (FAB<sup>+</sup>). Calcd for C<sub>26</sub>H<sub>32</sub>Co<sub>2</sub>S<sub>4</sub>: 590.00508. Found: 590.0046. <sup>1</sup>H NMR (CDCl<sub>3</sub>, 200 MHz, vs TMS):  $\delta$  1.93 (s, 30H, Cp\*), 8.30 (s, 2H, Ar). UV-vis (CH<sub>2</sub>Cl<sub>2</sub>):  $\lambda_{\max}/\text{nm}$  ( $\epsilon/\text{M}^{-1}\cdot\text{cm}^{-1}$ ) 307 (85 000), 677 (31 000). Anal. Calcd for C<sub>26</sub>H<sub>32</sub>Co<sub>2</sub>S<sub>4</sub>: C, 52.87; H, 5.46; S, 21.72. Found: C, 52.53; H, 5.60; S, 21.87.

**4a**. Mp: 206.5–207.5 °C. MS (FAB<sup>+</sup>): 482 ([M<sup>+</sup>], 100). HRMS (FAB<sup>+</sup>). Calcd for C<sub>22</sub>H<sub>31</sub>CoS<sub>4</sub>: 482.06406. Found: 482.0639. <sup>1</sup>H NMR (CDCl<sub>3</sub>, 200 MHz, vs TMS):  $\delta$  1.27 (d, *J* = 6.70 Hz, 12H, CHMe<sub>2</sub>), 1.95 (s, 15H, Cp\*), 3.40 (sp, *J* = 6.70 Hz, 2H, CHMe<sub>2</sub>), 7.83 (s, 2H, Ar). UV-vis (CH<sub>2</sub>Cl<sub>2</sub>):  $\lambda_{\max}/\text{nm}$  ( $\epsilon/\text{M}^{-1}\cdot\text{cm}^{-1}$ ) 300 (42 000), 613 (10 000). Anal. Calcd for C<sub>22</sub>H<sub>31</sub>CoS<sub>4</sub>: C, 54.74; H, 6.47. Found: C, 54.66; H, 6.39.

**Reaction of [Cp\*Co(CO)I<sub>2</sub>] with 3**. Benzo[1,2-*d*;4,5-*d'*]bis(1,3-dithiolane-2,6-dione) (**3**; 104 mg, 0.4 mmol) was treated with 4 equiv of <sup>t</sup>BuOK (180 mg, 1.6 mmol) in a THF solution (50 mL) at room temperature. A white cloudy solution was changed to a yellow cloudy one after 30 min. [Cp\*Co(CO)I<sub>2</sub>] (381 mg, 0.8 mmol) was added into this yellow solution. A purple solution was immediately obtained, and then the solution was further stirred for 30 min. After the solvent was removed under reduced pressure, the residue was extracted by dichloromethane/water and the organic layer was purified by column chromatography [silica gel; dichloromethane/petroleum ether, 2:1 (v/v)]. **4b** was obtained as a violet solid in 23% yield. MS (EI<sup>+</sup>, 70 eV): 424 ([M<sup>+</sup>]), 396 ([M<sup>+</sup>] – CO). HRMS (EI<sup>+</sup>, 70 eV). Calcd for C<sub>17</sub>H<sub>17</sub>CoOS<sub>4</sub>: 423.94943. Found: 423.9480. <sup>1</sup>H NMR (CDCl<sub>3</sub>, 200 MHz, vs TMS):  $\delta$  1.99 (s, 15H, Cp\*), 7.96 (s, 2H, Ar). UV-vis (CH<sub>2</sub>Cl<sub>2</sub>):  $\lambda_{\max}/\text{nm}$  ( $\epsilon/\text{M}^{-1}\cdot\text{cm}^{-1}$ ): 300 (45 000), 585 (11 000). Anal. Calcd for C<sub>17</sub>H<sub>17</sub>CoOS<sub>4</sub>: C, 48.10; H, 4.04. Found: C, 47.72; H, 4.01.

**5**. A suspension of **3** (5.16 g, 20 mmol) in dry MeOH (400 mL) was treated with a solution of sodium (2.1 g, 90 mmol) in dry

MeOH (60 mL). After stirring for 2 h, <sup>n</sup>Bu<sub>2</sub>SnCl<sub>2</sub> (12.15 g, 40 mmol) was added and the reaction stirred for 18 h. After evaporation under reduced pressure, the residue was extracted with CH<sub>2</sub>Cl<sub>2</sub>, and the solution washed with H<sub>2</sub>O, dried on MgSO<sub>4</sub>, and filtered on a short silica gel column (eluent: CH<sub>2</sub>Cl<sub>2</sub>). Recrystallization from CH<sub>3</sub>CN afforded light-yellow crystals (10.0 g) in 75% yield. Mp: 146–147 °C. <sup>1</sup>H NMR (CDCl<sub>3</sub>, 200 MHz, TMS):  $\delta$  0.94 (t, *J* = 7.2 Hz, Me, 12H), 1.40 (q, *J* = 7.2 Hz, 8H, CH<sub>2</sub>CH<sub>3</sub>), 1.69 (m, CH<sub>2</sub>, 16H), 7.56 (s, 2H, ArH). Anal. Calcd (found) for C<sub>22</sub>H<sub>38</sub>S<sub>4</sub>Sn<sub>2</sub>: C, 39.54 (39.92); H, 5.73 (5.75); S, 19.19 (19.49).

**Reaction of [Cp\*Co(CO)I<sub>2</sub>] with 5**. A THF solution (20 mL) of [Cp\*Co(CO)I<sub>2</sub>] (95 mg, 0.2 mmol) was added into the THF solution of **5** (134 mg, 0.2 mmol). The reaction mixture was stirred for 3 h at room temperature. The solvent was evaporated under reduced pressure, and the residue was separated by column chromatography on silica gel. The monocobalt complex **4c** was eluted by dichloromethane/petroleum ether [2:1 (v/v)], and the dicobalt complex **1** was obtained from dichloromethane elution. **4c** and **1** were isolated as blue solids in 21% and 50% yields, respectively. The reaction of 2 equiv of [Cp\*Co(CO)I<sub>2</sub>] (190 mg, 0.4 mmol) with **5** (134 mg, 0.2 mmol) under the same conditions as those above afforded the dinuclear complex **1** in 78% yield.

**4c**. Mp: 100.5–101.5 °C. MS (FAB<sup>+</sup>): 630 ([M<sup>+</sup>], 100). HRMS (FAB<sup>+</sup>). Calcd for C<sub>24</sub>H<sub>35</sub>CoS<sub>4</sub>Sn: 629.99756. Found: 629.9967. <sup>1</sup>H NMR (CDCl<sub>3</sub>, 200 MHz, vs TMS):  $\delta$  1.35–1.75 (m, 18H, Bu), 1.99 (s, 15H, Cp\*), 7.98 (s, 2H, benzene). UV-vis (CH<sub>2</sub>Cl<sub>2</sub>):  $\lambda_{\max}/\text{nm}$  ( $\epsilon/\text{M}^{-1}\cdot\text{cm}^{-1}$ ) 253 (22 000), 301 (36 000), 637 (10 000). Anal. Calcd for C<sub>24</sub>H<sub>35</sub>CoS<sub>4</sub>Sn: C, 45.80; H, 5.60. Found: C, 45.01; H, 5.61.

**[Cp\*Co(bdt)] (6)**. Benzo[*d*]-1,3-dithiolane-2-one (**7**; 101 mg, 0.6 mmol) was treated with 2 equiv of <sup>t</sup>BuOK (135 mg, 1.2 mmol) in a THF solution (30 mL) at room temperature. A white cloudy solution was changed to a yellow cloudy one after 30 min. [Cp\*Co(CO)I<sub>2</sub>] (286 mg, 0.6 mmol) was added into this yellow solution. A purple solution was immediately obtained, and then the solution was further stirred for 30 min. After the solvent was removed under reduced pressure, the residue was extracted by dichloromethane/water and the organic layer was purified by column

chromatography [silica gel; dichloromethane/petroleum ether, 2:1 (v/v)]. **6** was obtained as a violet solid in 59% yield. Mp: 242–243 °C. MS (FAB<sup>+</sup>): 334 ([M<sup>+</sup>]). HRMS (EI<sup>+</sup>). Calcd for C<sub>16</sub>H<sub>19</sub>CoS<sub>2</sub>: 334.02602. Found: 334.0276. <sup>1</sup>H NMR (CDCl<sub>3</sub>, 200 MHz, TMS): δ 2.01 (s, 15H, Cp\*), 7.13 (dd, *J* = 3.2 and 6.1 Hz, 2H, benzene), 7.90 (dd, *J* = 3.2 and 6.1 Hz, 2H, benzene). UV–vis (CH<sub>2</sub>Cl<sub>2</sub>): λ<sub>max</sub>/nm (ε/M<sup>-1</sup>·cm<sup>-1</sup>) 574 (8600), 448 (1400), 298 (29 000). Anal. Calcd for C<sub>16</sub>H<sub>19</sub>CoS<sub>2</sub>: C, 57.47; H, 5.73. Found: C, 57.38; H, 5.74.

**Reaction of 8 with P(OMe)<sub>3</sub>.** Excess P(OMe)<sub>3</sub> (59 μL, 0.5 mmol) was added into a dichloromethane solution (5 mL) of [Cp\*Co(dmit)] (20 mg, 0.05 mmol). The initially green solution rapidly changed to dark red. The reaction mixture was stirred for 5 min. The product was directly crystallized by vapor diffusion of pentane at 0 °C. The excess P(OMe)<sub>3</sub> was removed by filtration and washing with pentane. Brown crystals of [**8**·P(OMe)<sub>3</sub>] were obtained in 99% yield. MS (FAB<sup>+</sup>): 514 ([M<sup>+</sup>]). <sup>1</sup>H NMR (CDCl<sub>3</sub>, 200 MHz, vs TMS): δ 1.51 (d, *J*<sub>P-H</sub> = 2.7 Hz, 15H, Cp\*), 3.87 (d, *J*<sub>P-H</sub> = 9.7 Hz, 9H, OMe). The <sup>1</sup>H NMR spectrum was obtained in a CDCl<sub>3</sub> solution of complex **8** in the presence of 1000 equiv of P(OMe)<sub>3</sub>. UV–vis (CH<sub>2</sub>Cl<sub>2</sub>): λ<sub>max</sub>/nm (ε/M<sup>-1</sup>·cm<sup>-1</sup>) 282 (25 000), 340 (15 000), 529 (8400). The UV–vis spectrum was measured in the presence of 2000 equiv of P(OMe)<sub>3</sub>. Anal. Calcd for C<sub>16</sub>H<sub>24</sub>CoO<sub>3</sub>PS<sub>5</sub>: C, 37.34; H, 4.70. Found: C, 37.80; H, 4.67.

**Reaction of 1 with P(OMe)<sub>3</sub>.** Excess P(OMe)<sub>3</sub> (10 drops) was added into the chloroform solution (10 mL) of [Cp\*Co(bt)CoCp\*] (18 mg, 0.03 mmol). The initial blue solution was rapidly changed to greenish brown. The reaction mixture was stirred for 30 min. A product was directly crystallized from vapor diffusion of pentane at 0 °C. The excess P(OMe)<sub>3</sub> was removed by filtration and washing with pentane. Brown crystals of [**1**·P(OMe)<sub>3</sub>] were obtained in 90% yield. MS (FAB<sup>+</sup>): 714 ([M<sup>+</sup>]). <sup>1</sup>H NMR (CDCl<sub>3</sub>, 200 MHz, vs TMS): δ 1.52 (d, *J*<sub>P-H</sub> = 2.6 Hz, 15H, Cp\*), 2.00 (s, 15H, Cp\*), 3.68 (d, *J*<sub>P-H</sub> = 9.7 Hz, 9H, OMe), 7.72 (s, 2H, benzene). The <sup>1</sup>H NMR spectrum was obtained in a CDCl<sub>3</sub> solution of complex **1** in the presence of 1000 equiv of P(OMe)<sub>3</sub>. Anal. Calcd for C<sub>29</sub>H<sub>41</sub>Co<sub>2</sub>O<sub>3</sub>PS<sub>4</sub>: C, 48.73; H, 5.78. Found: C, 48.44; H, 5.48. UV–vis–NIR (CH<sub>2</sub>Cl<sub>2</sub>): λ<sub>max</sub>/nm (ε/M<sup>-1</sup>·cm<sup>-1</sup>) 301 (56 000), 856 (13 000). The UV–vis–NIR spectrum was measured in the presence of 2000 equiv of P(OMe)<sub>3</sub>.

**X-ray Diffraction Studies.** The single crystals of complexes **1**, **6**, [**1**·P(OMe)<sub>3</sub>], and [**8**·P(OMe)<sub>3</sub>] were obtained by vapor diffusion of pentane into a dichloromethane or chloroform solution at 0 °C. Single crystals of complex **4a** were obtained from hot EtOH. Crystals were mounted on the top of a thin glass fiber. Data were collected on a Nonius Kappa CCD diffractometer for complexes [**1**·P(OMe)<sub>3</sub>] and [**8**·P(OMe)<sub>3</sub>] at room temperature or a Bruker AXS SMART APEX CCD diffractometer for complexes **1**, **4a**, and **6** at

100 K with graphite-monochromated Mo Kα radiation (λ = 0.710 73 Å). Structures were solved by direct methods (SHELXS-97) and refined (SHELXL-97)<sup>58</sup> by full-matrix least-squares methods, as implemented in the WinGX software package.<sup>59</sup> Absorption corrections were applied. H atoms were introduced at calculated positions (riding model), included in structure factor calculations, and not refined. Crystallographic data of complexes are summarized in Table 6.

**CV Measurements.** All electrochemical measurements were performed under an argon atmosphere. Solvents for electrochemical measurements were dried by 4 Å molecular sieves before use. A Pt wire served as the counter electrode, and the reference electrode, SCE (saturated calomel electrode), was corrected for junction potentials by being referenced internally to the ferrocene/ferrocenium (Fc/Fc<sup>+</sup>) couple. A stationary Pt disk (1.0 mm in diameter) was used as the working electrode. CV measurements were performed with an Autolab PGSTAT 20 potentiostat from Eco Chemie BV, equipped with General Purpose Electrochemical System GPES software (version 4.5 for Windows). Solution resistance was compensated for by positive feedback. Dichloromethane solutions (1 mmol·dm<sup>-3</sup>) of dithiolenes complexes containing 0.1 mol·dm<sup>-3</sup> tetrabutylammonium hexafluorophosphate (NBu<sub>4</sub>PF<sub>6</sub>) at 25 °C were used for measurements.

**Determination of Formation Constants (K) for the P(OMe)<sub>3</sub> Adduct of Cp\*Co Dithiolenes Complexes.** Dichloromethane solutions of complex **1** (*c* = 2.5 × 10<sup>-5</sup> mmol·dm<sup>-3</sup>), **4b**, **6**, and **8** (*c* = 5.0 × 10<sup>-5</sup> mmol·dm<sup>-3</sup>) were precisely prepared. The UV–vis–NIR spectral changes were measured in the presence of different concentrations of P(OMe)<sub>3</sub>. The formation constant (*K*) was determined by literature methods.<sup>26b</sup>

**Acknowledgment.** We thank Thierry Roisnel (Centre de Diffractométrie, Rennes) for the X-ray data collections. We also thank the Ministère de la Recherche (France) and the ANR (France) (CHIRASYM project) for a postdoctoral grant (to M.N.).

**Supporting Information Available:** X-ray crystallographic files in CIF format for complexes **1**, **4a**, **6**, [**1**·P(OMe)<sub>3</sub>], and [**8**·P(OMe)<sub>3</sub>]. This material is available free of charge via the Internet at <http://pubs.acs.org>.

IC700778B

(58) Sheldrick, G. M. *SHELX97—Programs for Crystal Structure Analysis*, release 97-2; University of Göttingen: Göttingen, Germany, 1998.

(59) Farrugia, L. J. *J. Appl. Crystallogr.* **1999**, *32*, 837.